# Pinning the timing of deglaciation of the Western Foxe Peninsula, Baffin Island, Nunavut

**Samuel Kelley**
**Department of Earth Sciences**
**Dalhousie University**

**Advisor: Dr. John Gosse**
**Department of Earth Sciences**
**Dalhousie University**

Submitted in partial fulfillment of the requirements for the Degree of Honours Bachelor of Science Earth Sciences
Dalhousie University, Halifax, Nova Scotia

DALHOUSIE UNIVERSITY
*Inspiring Minds*

**Department of Earth Sciences**
Halifax, Nova Scotia
Canada B3H 4J1
(902) 494-2358
FAX (902) 494-6889

DATE: April 27, 2007

AUTHOR: Samuel Edward Kelley

TITLE: Pinning the timing of deglaciation of the western Foxe Peninsula, Baffin Island, Nunavut

Degree: B.Sc. Convocation: May 2007 Year: 2007

Permission is herewith granted to Dalhousie University to circulate and to have copied for non-commercial purposes, at its discretion, the above title upon the request of individuals or institutions.

Signature of Author

THE AUTHOR RESERVES OTHER PUBLICATION RIGHTS, AND NEITHER THE THESIS NOR EXTENSIVE EXTRACTS FROM IT MAY BE PRINTED OR OTHERWISE REPRODUCED WITHOUT THE AUTHOR'S WRITTEN PERMISSION.

THE AUTHOR ATTESTS THAT PERMISSION HAS BEEN OBTAINED FOR THE USE OF ANY COPYRIGHTED MATERIAL APPEARING IN THIS THESIS (OTHER THAN BRIEF EXCERPTS REQUIRING ONLY PROPER ACKNOWLEDGEMENT IN SCHOLARLY WRITING) AND THAT ALL SUCH USE IS CLEARLY ACKNOWLEDGED.

**ABSTRACT**

The Kingnait Moraine system in western Foxe Peninsula, Baffin Island marks the ice margin position before the final wasting of glacial ice in the area. This area of Baffin Island is of particular interest due to its proximal location to both the Hudson Strait and the Foxe Basin, two locations which controlled local ice dynamics. Ice movement in this region also may have major implications for Heinrich Events in the north Atlantic region. Cosmogenic $^{10}$Be exposure dating was used to date both boulders perched on esker crests as well as a depth profile taken through the topsets of a glaciomarine delta at 151 m asl. Boulder exposure ages on eskers crests, bracketing the moraine, yield maximum ages of $8.9 \pm 0.5$ ka and $6.9 \pm 0.4$ ka (2 $\sigma$ precision) indicating that the moraine was likely formed following the Cockburn event (9.6 ka) though possibly in response to the 8.2 Arctic cooling event or the Noble inlet advance (8.9-8.4 ka). This agrees with a mean exposure age of $7.5 \pm 1.4$ ka for the abandonment of a sampled glaciomarine delta approximately 80 km to the southeast, which is down ice from the moraine. The exposure ages represent the first known esker exposure ages and demonstrate an important advancement in delta chronologic technique. Recent $^{14}$C ages of marine shells (Utting et. al., in press Feb., 2007) further support this conclusion.

**Keywords:** *Moraine, Esker, Cosmogenic Nuclide, Glaciomarine Delta, Ice Stream*

## TABLE OF CONTENTS

## FIGURES

## TABLES



## APPENDICES

**Acknowledgments**

I would like to thank my advisor, John Gosse for all his generous support in all aspects of this project. I would also like to thank Dan Utting for providing invaluable assistance in so many facets of this project. I would like to thank Doug Hodgson for his lending his experienced eye to this project as well as his assistance in sample collection. Further, I'd like to commend Guang Yang who tirelessly guided me through the chemistry process, and is greatly responsible for the great data presented in this study. I would additionally like to thank the members of the SWBIG team who provided multifaceted advice as well as personal guidance, especially Michelle Trommelen for her assistance with air photos, Marc St. Onge for his tireless enthusiasm, Kerry Brazel for digital support, and Jamie Bowles, our helicopter pilot. Finally, I would like to thank my classmates, roommates, and girlfriend for their constant tolerance with me, and assistance in maintaining a certain degree of sanity throughout the duration of this project.

# 1.0 Introduction

The Greenland ice stratigraphic record of climate change since the last glaciation has revealed significant high amplitude, high frequency departures from normal (Meese et. al., 1994; Dansgaard et. al., 1993). The timing and extent of these climate variations have also been documented in numerous other northern climate proxy records, such as lake and marine sediment cores. However, conversion of these proxy records to temperature or precipitation time series is difficult due to inherent problems in interpreting each of the records. Moraines mark the position of a glacier margin at some instance in time. When dated, the record of aerial ice extents can be used to provide temperature or precipitation information through relatively simple mass balance relationships (Reuther et. al., 2006). A complication is that because there was so much climate variability during the late Pleistocene and Holocene, there are often numerous moraines preserved, and without knowing their age precisely a link cannot be formed between a feature and specific climate event.

An opportunity to map and date moraines on the Foxe Peninsula, southern Baffin Island, was afforded in 2006 during a summer field program by the Geologic Survey of Canada (GSC) and Canada-Nunavut Geoscience Office (C-NGO) organizations. The Foxe Peninsula is in a pivotal position to study the history of deglaciation in the area because it is a transition zone abutted by two important glaciological regimes: Hudson Strait Ice Stream and Foxe Basin Ice Centre (Fig. 1.1).

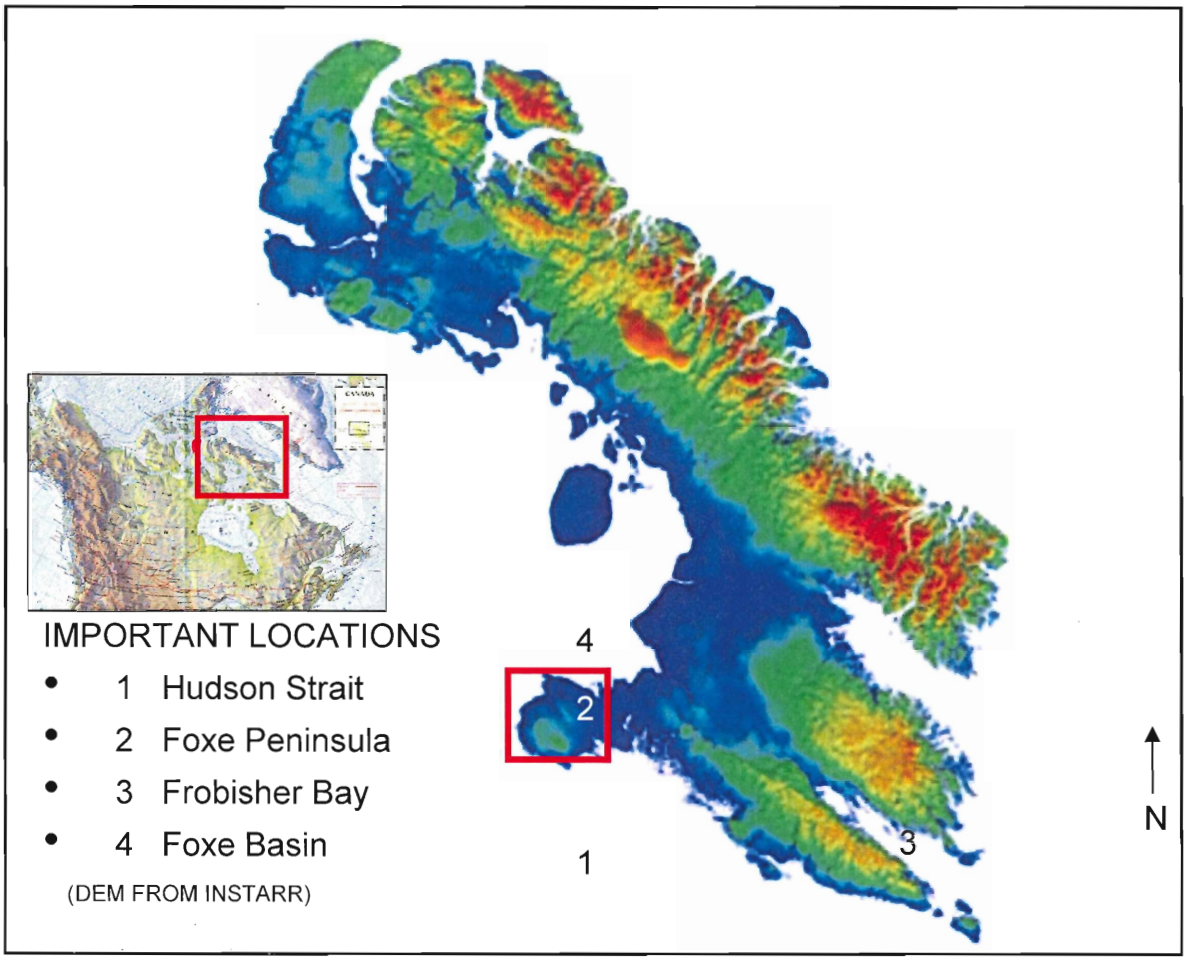


Figure 1.1: Location map. Red box is the study area, with numbers referring to physiographical features.

Large moraines, height greater than 5 m, on Baffin Island have traditionally been interpreted to represent the Cockburn age cold period, 9.6 ka (Andrews, 1978; Blake, 1966). However, three other significant climate events occurred in a relatively short time: the Younger Dryas (12.8-11.5 ka) (Taylor et al, 1997), the Noble Inlet advance (8.9-8.4 ka) (Miller et al, 1988; Jennings et al, 1998), and the 8.2 ka cold event (Miller et al., 2005;Borgstom, 2001; Grafenstein et. al., 1998). No moraines have been dated on the Foxe Peninsula, despite some of them having been mapped previously and used to help interpret the glacial dynamics responsible for the deglaciation of the central Arctic and even Heinrich events (marine sedimentological records of periods of significant iceberg

discharges from Hudson Strait and elsewhere) (Blake, 1966). In general, due to a lack of radiocarbon datable material, chronology of Quaternary terrestrial landforms on Baffin Island is rare.

The moraines, locally named the Kingnait Mountains, meaning "saw-blade-like" in Inuktitut, henceforth will be referred to as the Kingnait moraines. An interesting feature of these moraines is their close proximity to multiple eskers. The most important relationship between these two types of glacial features is the fact that the eskers cross the moraines. During ice marginal retreat the esker was sequentially uncovered, and thus exposed to cosmic rays. During retreat or advance of an ice margin moraines can be deposited, as a result of lowering temperatures or increase precipitation. The Kingnait moraines are hypothesized to be of Cockburn age, 9.6 ka, primarily due to their size, which is significantly larger than any other glacial feature in the area (Blake, 1966). This hypothesis is based on the fact that the Cockburn sub-stage is considered responsible for all other moraines of similar size to the Kingnait moraines in the region, as well as that the orientation of the Kingnait moraines is fairly similar to moraines dated to be of Cockburn age near Frobisher Bay (Figure 1.1) to the east of Foxe Peninsula (Blake, 1966). The moraines are unlikely to represent the Younger Dryas event, due to the fact that Younger Dryas moraines in Canada have been found much further to the south around the Great Lake (Lowell et al., 1999). It is also unlikely that the moraines represent the 8.2 ka event, because of a lack of landforms of similar size connected to this climate event (Long et al., 2006).

In this study the proposed hypothesis that the Kingnait Moraines are of Cockburn age has been tested by first mapping the extent of the moraines, and then dating the

moraines. First, to ascertain the full extent of the moraines, the area was mapped using a combination of air photos, as well as field checking of selected sites, and a brief sedimentological study of the surficial deposits present in the region. Ice dynamics in the research area were the focus of the C-NGO program for 2006 which relied on using various ice flow indicators, such as striae, grooves, as well as paleo-flow measurements within the eskers. The ice margin was then dated using terrestrial cosmogenic nuclide (TCN) measurements on boulders found on esker crests and topset sediments on a raised glaciomarine delta.

# 2.0 Background

## *2.1 Regional background*

The study area is on the Foxe Peninsula, Southwestern Baffin Island (Figure 2.0). The Foxe Peninsula is bounded to the north by Foxe Basin and to the west and south by Hudson Strait, and lies approximately between 65° 30 N and 64° 00 N. The 2500 $km^2$ study area occupies the western half of the Foxe Peninsula, between latitudes 65° 00 and 64°30 N and longitudes 78°00 to 76°00 W. A major physiographical feature in the region is the Cape Dorset upland, an area of high relief hills of Archean metamorphic bedrock. The maximum relief is 250 m due to a combination of both fluvial and glacial incision. Relief diminishes northward as the bedrock is covered by thickening Quaternary sediments that create a low relief plane with an elevation ranging from 180 to 120 m asl. There is a general west to east slope through the region with a gradient of 0.01 m/km across the field area.

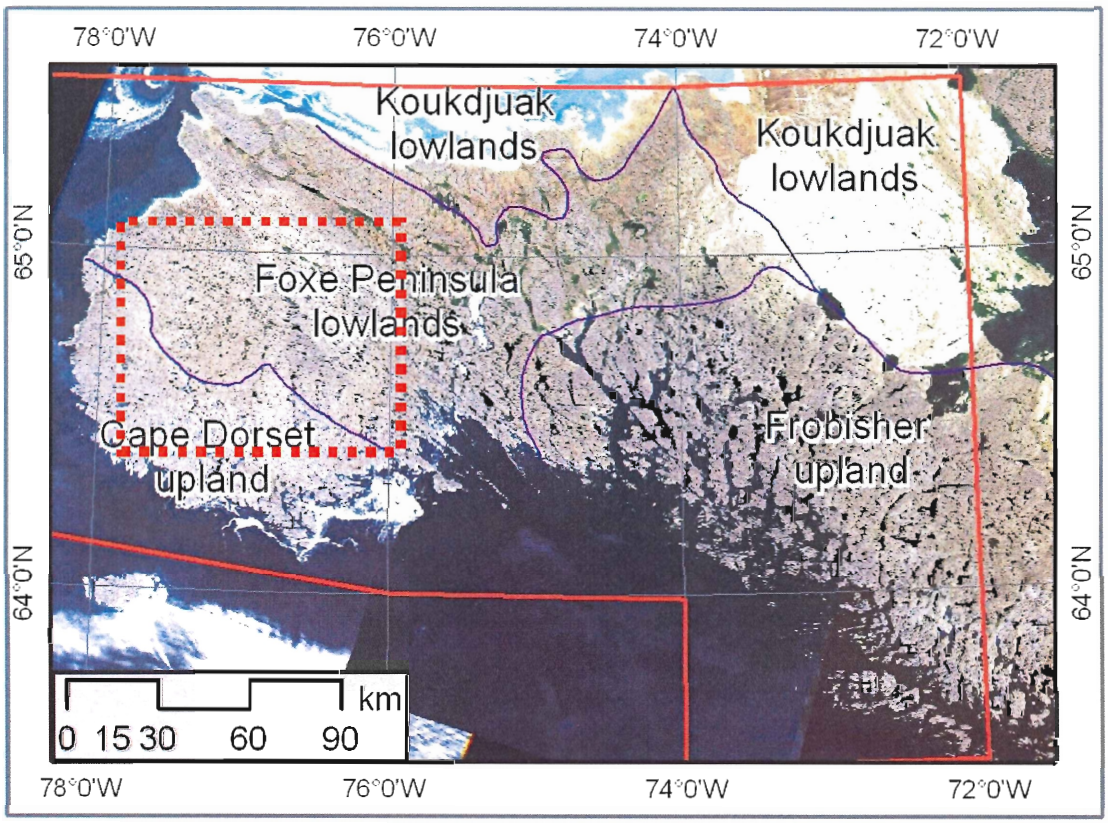


Figure 2.1: Map of the Foxe peninsula highlighting the major physiographical regions. (Dashed Red box = approximate field area) (Utting et. al., 2007)

Climatic data for Baffin Island is sparse with only a short term (30 year) record available from Cape Dorset, which is on the coast, approximately 15 km south of the study area. Average annual temperature for Cape Dorset is -9.3° C with the monthly range of -26°C to 7.4° C (Environment Canada, 2000). Precipitation in the form of snow has been recorded to fall year round with the majority falling between October and May. The total average snowfall for the region is 296.6 cm per year. Rain falls primarily from June to September, with the average yearly total rainfall being 14.4 cm over the past 30 years. With average temperatures below freezing, permafrost is prevalent throughout the study area, although the thickness or depth is not precisely known. Sea ice is common in

the oceans surrounding the peninsula with ice currently remaining in Foxe Basin well into July (Environment Canada, 2000).

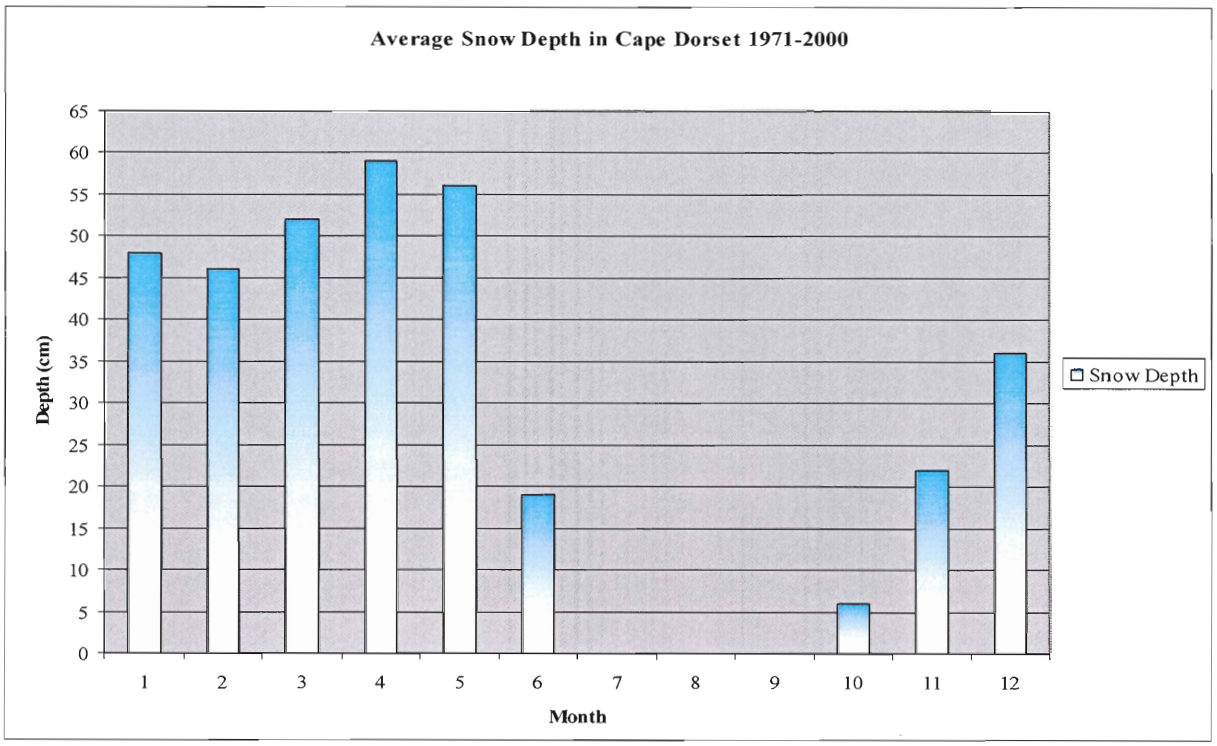


Figure 2.2: Yearly snow depth averages for Cape Dorset, Nunavut (Environment Canada, 2000)

In terms of bedrock, the western Foxe Peninsula is cored by the Lake Harbour group, a clastic/carbonate sequence, approximately 1.9 Ga. This Archean segment is one of many pieces which were accreted together as a part of the Trans-Hudson Orogen. The Foxe Peninsula is considered part of the Rae province. Structurally, the metamorphic sequences of the Foxe Peninsula are heavily deformed by collisions which initially produced this orogenic belt (St. Onge, 1999).

The surficial geology of the study area is dominated by a mixture of tills and glacial fluvial sediments forming a wide range of geomorphic features. The two most dominant landforms inland are eskers and moraines, but fluvial terraces and glaciolacustrine landforms are common as well. Raised marine beaches as well as

glaciomarine deltas occur mostly within 20 km of the coast. Moraines in the study area are distinguished from eskers by their composition, primarily the presence of till as well as their relatively wider asymmetric appearance in relation to eskers. Eskers here tend to be narrower and more sinuous than the moraines, as well as appearing triangular in cross section. Besides morphology the primary method for identifying moraines was grain size analysis, with eskers lacking silt and clay fractions as based on observations made in the field.

| **Glacial Landform** | **Sediment composition** | **Physical appearance** | **Position of creation (Glacial)** | **Comments** |
|---|---|---|---|---|
| Esker | Sand to boulders. Can be stratified. | Sinuous ridges. Triangular cross section. | Resulting from streams depositing sediments in tunnels inside of the ice body. | Form roughly parallel to ice flow. |
| Moraine | Any grain size from silt to boulders. No sediment structures. | Non-symmetrical cross section. Slightly more linear than eskers. | The result of material being pushed up in front of an advancing ice margin or abandoned by a retreating ice margin. Feature is abandoned when retreat occurs. | Generally larger in volume than esker, also may have very little vertical relief. |
| Glaciomarine Delta | Silt to gravels. Stratified. | Wedge shaped with flat top. Generally steep sided at base. | Formed at the contact between an ice margin and the ocean, where sediment from the ice body is deposited in a marine environment. | Characterized by flat top and stratified sediment deposits. |

Table 1.1: Description of three glacial landforms of importance to this project.

Ice flow indicators suggest that flow of the most recent ice in the study area was roughly from the north, out of the Foxe Basin (Utting et. al., 2007). These measurements were taken a variety of ways, with striae and grooves on exposed bedrock being the most common, though other features, such as de geer moraines, the asymmetry of end moraines, and pebble imbrication in eskers were also contributing factors (Utting et. al., 2007).

The Quaternary deposits within the study area were classified using the criteria from the Southwest Baffin Integrated Geoscience project (SWBIG) in which I participated. In the region unconsolidated Late Pleistocene or Holocene material was dominated by glaciomarine sediment, glaciofluvial sediment, and till. Glaciomarine material is defined as sediments deposited during a period of a higher sea level. This typically is fine sand, silt, clay and stony mud. Other materials classified as glaciomarine are raised beach sediments and glaciomarine delta sediments. Glaciofluvial material is defined as having been deposited by melt-water in front of or under a glacier, and is characterized by sorted stratified gravels and sand. Till is defined as being deposited in sub-glacial to ice-marginal environments, and can be composed of any mixture of sediment, but usually a dimicton in this region.

The presence of such well defined glacial landforms is the reason why this area was selected for study, and is the result of geologically recent ice movement across the region. There are two interesting locations in the context of local ice dynamics. The first being the Hudson Strait, which contained a fast flowing ice stream that flowed to the southeast from the main body of the Laurentide Ice Sheet (Borgstrom, 2001). The second "interesting" location is the Foxe Basin, which contained an ice dome during the period of glaciation of the region, and is likely the source for ice flowing across the peninsula (Dyke, 2006). The contrast between the fixed ice dome in the northeast and the high velocity ice stream to the south and west creates a highly sensitive transition location in which the study area falls. This context makes the study area for this project a very interesting location to study ice dynamics.

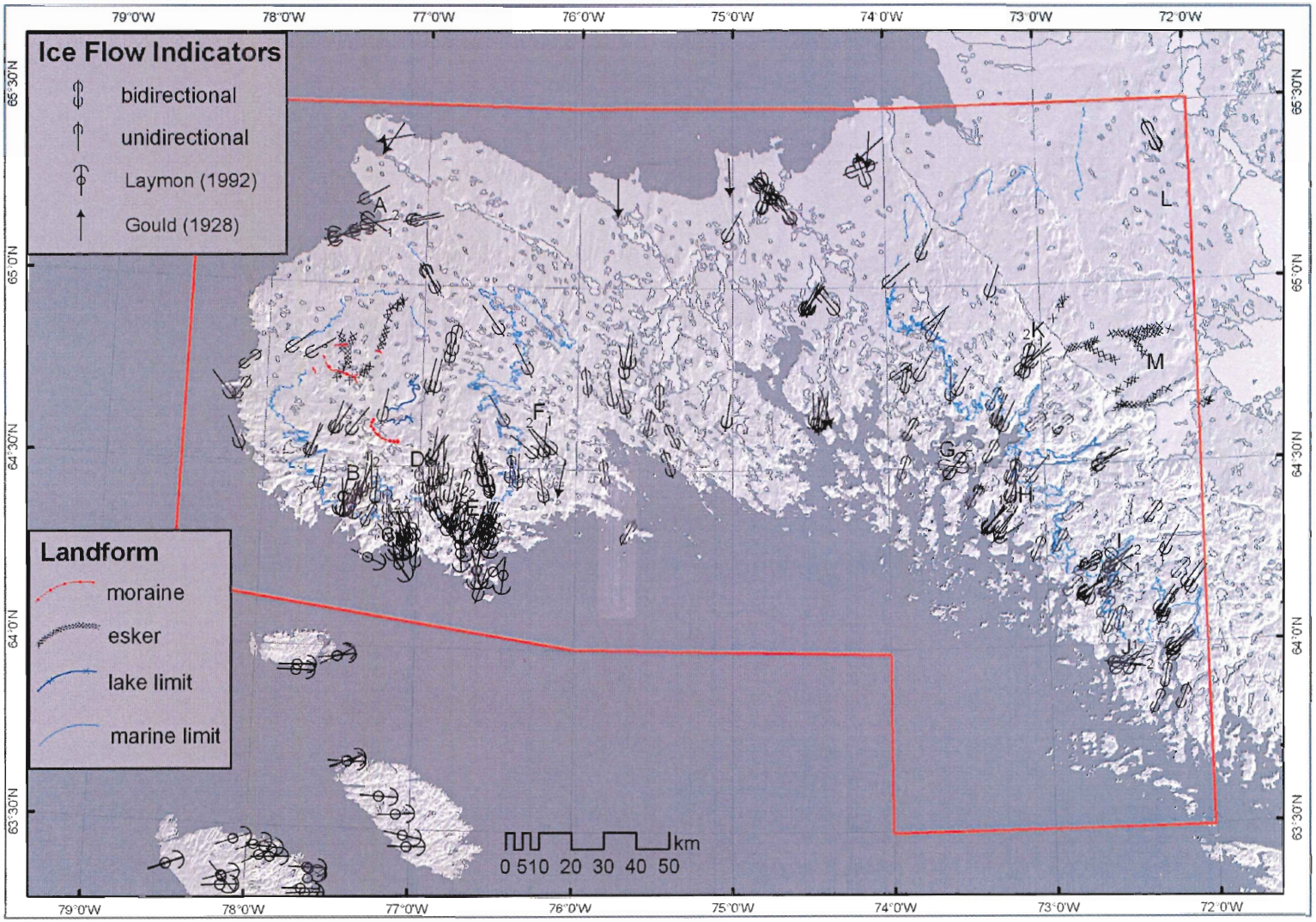


Figure 2.3: This map shows ice flow measurements collected during the 2006 SWBIG field season; note general flow to the south in the western portion of the peninsula (Utting, 2007)

During one of the earliest studies of ice dynamics, Bell (1885) noted striae on Big Island in the Hudson Strait south of the Foxe Peninsula. All of the striae found were trending to the southeast, nearly parallel to the strait. Bell (1901) later noted striae at 165° along the Baffin coast, which matched data from the rest of Baffin Island. This was later interpreted to be the result of tributary flow into the strait from inland Baffin Island. Also in 1901, Bell noted a distinct transition at 90 m asl on Big Island, below which bare rock and raised beaches were prevalent, contrasting with loose angular rock above. This change in ground cover marks a washing limit and represents the limit of local sea level rise known as the marine limit.

The only other detailed glacial geomorphology completed on the Foxe Peninsula was done by Blake (1966). Blake's mapping of the region was predominantly performed using air photos, though some field work was conducted, primarily in the eastern part of the Peninsula. The nature of the Kingnait moraines was unclear to Blake, who identified them as possible moraines or eskers. On a more regional scale Blake concluded that moraines found near Frobisher Bay may be correlative to the Kingnait moraines. But Blake suggested that the Kingnait moraines may have been deposited approximately 8.0 ka, when he believed that the Hudson Strait was opened. Blake concluded that due to sea level rise western Foxe Peninsula was an island around the time period of $6.4 \pm 0.3$ ka, based on calibrated radiocarbon analysis of marine shells found there (Blake, 1966; Stuiver, 1992, 2005).

From 1970 to the present time, research from the Institute of Arctic and Alpine Research further raised the level of understanding regarding climate change in southern and eastern Baffin Island, and provide useful insight to processes that may have also

occurred on the Foxe Peninsula. The findings of this group include evidence for an Ice Stream occupying the Hudson Strait from 14 to 8 ka and discovery of a glacial advance across the Hudson Strait onto Baffin Island from the west. This advance occurred from 9.9 to 9.6 ka, and is known as the Gold Cove advance (Kaufman et al., 1993; Jennings et. al., 1998).

One of the most comprehensive studies in the region was recently published by the Geologic Survey of Canada (Hodgson, 2005). Hogdson studied the nearby Meta Incognita Peninsula and found evidence both for flow down the Hudson Strait, as well as for flow of ice southeast from the Foxe Basin. Hodgson found evidence that ice retreat occurred at 8.9 ka, with ice retreating on land from Frobisher Bay, as well as ice moving seaward into the Hudson Strait around 8.4 ka, though the relationship between onshore and Hudson Strait ice remains fairly unclear.

Despite extensive work on both surficial geology and glacial dynamics, a geochronologic history for the Foxe Peninsula is yet unknown. This lack of data is partly due to the remoteness of the region, as well as a lack of suitable material for radiocarbon dating. The development of terrestrial cosmogenic nuclides (TCN) exposure dating techniques since the mid-1980s recently allows for the dating of Holocene exposures. This has made it possible to decipher a chronologic record for this important transitional locality.

## *2.2 Terrestrial cosmogenic nuclide principles*

The dating method employed in this project utilizes TCN to determine the duration of time that a landform surface is exposed to cosmic radiation. TCN are the result of interactions between cosmic radiation and nuclei of exposed target atoms in

materials in the upper few meters of the Earth's surface. In the field of TCN exposure dating there are six commonly used nuclides: $^{10}Be$, $^{26}Al$, $^{36}Cl$, $^{14}C$, $^{3}He$, and $^{21}Ne$, with the latter two being stable noble gases.

The production of cosmogenic nuclides, both terrestrial and atmospheric, begins with interactions between primary galactic cosmic radiation (GCR). GCR is a combination of high energy particles (mostly 1-1000 GeV), composed of 85% protons, 14% α-particles, 3% electrons, and 1% heavier nuclei (Smart and Shea, 1985; Lal, 1988). These particles originate primarily from the Milky Way galaxy and while many are repelled by the Earth's magnetic field, some do penetrate the field (Gosse and Phillips, 2001). GCR first interacts with the atmospheric nuclei, causing a cascade of secondary particles (neutrons, $\pi^{\pm}$ and $K^{\pm}$ mesons) (Gosse and Phillips, 2001). In the case of this project, the majority of TCN production is due to spallation, resulting from interactions between high energy nucleons which break up the target nuclei. Another contributor to production is muons, which result from the decay of mesons that do not react immediately with the atmosphere (mesons have a $10^{-6}$ second lifetime). $^{10}Be$, the nuclide used in this study, is produced primarily through the spallation of Si and O in quartz ($SiO_2$) (Gosse and Phillips, 2001)

This production of $^{10}Be$ can also occur before the sampled material was buried; therefore there can be a significant concentration of $^{10}Be$ in the sample when the shielding material, in this project ice, is removed. The additional $^{10}Be$ is known as inheritance. This is subtracted from the total concentration. The adjusted concentration can then be used with the site production rate to date the exposure history of a rock or

sediment surface. This exposure time in terms of this project is the time since ice retreated from above the sampled location.

# 3.0 Methods

During the summer of 2006 I participated as a member of the C-NGO surficial field mapping party in southwestern Baffin Island, and contributed to the surficial mapping of the entire Foxe Peninsula. The following methodology regards my own work on the moraines and eskers of my field area.

## *3.1 Air photo mapping*

Air photos were inspected at a 1:60,000 scale to identify large scale landforms as well as features that were too large or too subtle to be seen from the ground. This information was then used to plan daily traverses. Mapping moraines, eskers, deltas, and glaciofluvial terraces allowed the measurement of their orientation and extent. The orientation of moraines and eskers provided a regional sense of ice flow direction while the extent of the landforms provides insight into the size of the contemporaneous ice mass. In addition to mapping, air photo examination allowed for a more focused search for sampling locations (See Appendix A).

## *3.2 Geochronology*

In this project different techniques were employed: depth profiles to date glaciomarine deltas and boulder surface ages to date eskers.

### 3.2.1 Glaciomarine deltas

Chronology of glaciomarine deltas provide ages and rates for ice retreat, as well as information about on glacial isostacy, due to the formation of the topset-foreset contact at the contemporaneous sea level. The keys to a good glaciomarine delta sample site are that it is close to marine limit and well preserved (not eroded). By knowing that the delta was near or at local marine limit, one can infer that the delta was exposed shortly after ice

retreated. Also, it can be assumed that the delta remained sub-aerially exposed and was not covered by subsequent transgression. Preservation of the delta is important so the material has remained roughly at the same vertical position in the deltaic sequence, and thus the partial shielding of each subsurface sample from cosmic rays has remained constant since deposition. Our sampling technique involves the digging of a sample pit in the center and least disturbed portion of the delta. The pit was 1 x 2 m wide and 1.5 m deep. Samples were taken in the top 1 m of the delta to provide a suite of representative TCN concentrations through topset beds. The first sample consisted of pebbles from the delta surface. These pebbles likely represent a lag deposit resulting from wind deflation of the topset beds. Alternatively, the pebbles may have been cryoturbated or heaved to the surface. This is less likely due to the lack of mud boils present on the delta surface, a feature usually connected to cryoturbation in the area. Planar beds were also visible below the mixing layer which was created by bioturbation, further suggesting a lack of cryoturbation. The other samples taken at approximately 20 cm intervals consisted of sand collected in 3-6 cm thick bands, with the top 20 cm not sampled due to possible cryogenic or biological turbation. This is important to our study because turbation takes material out of its vertical position thus changing the cosmic ray flux, therefore changing the production rate for any $cm^3$ in the mixing zone, although the integrated production rate through the entire mixed zone would be the same on the as the same thickness of an unmixed zone. The samples weighed approximately 0.8 kg and consisted of sand to pebbly sand (Fig 3.2).

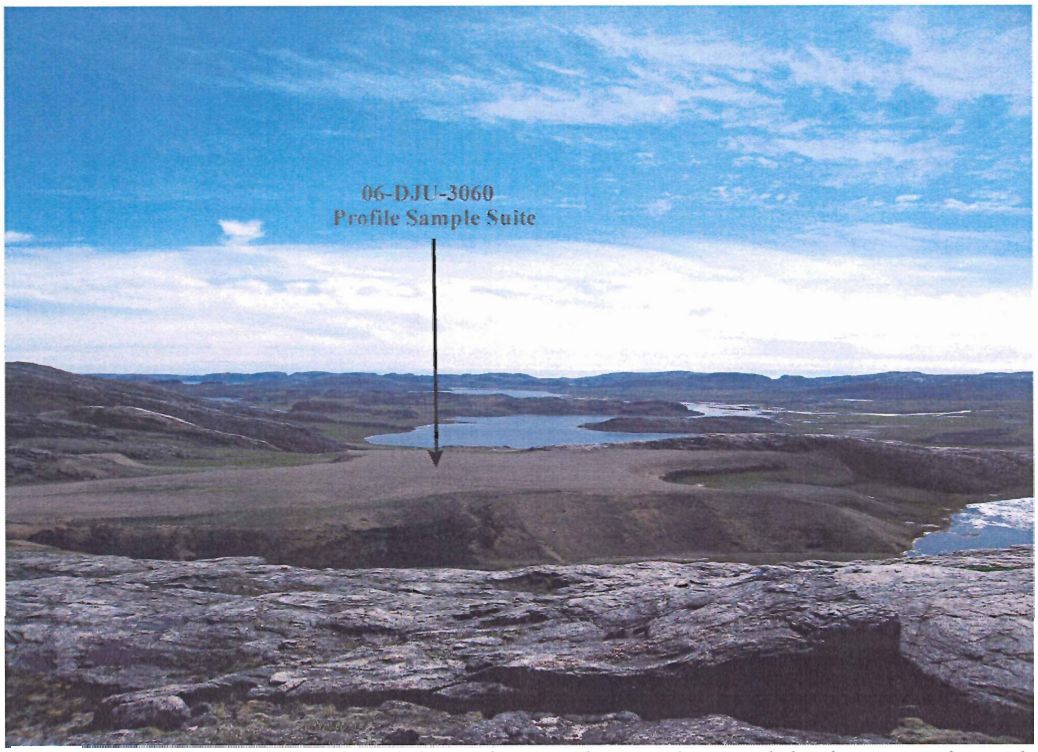

Figure 3.1: Sampled glaciomarine delta. View to the southeast; delta is approximately 100 m wide and 15 m higher than surrounding terrain (S. Kelley photo).

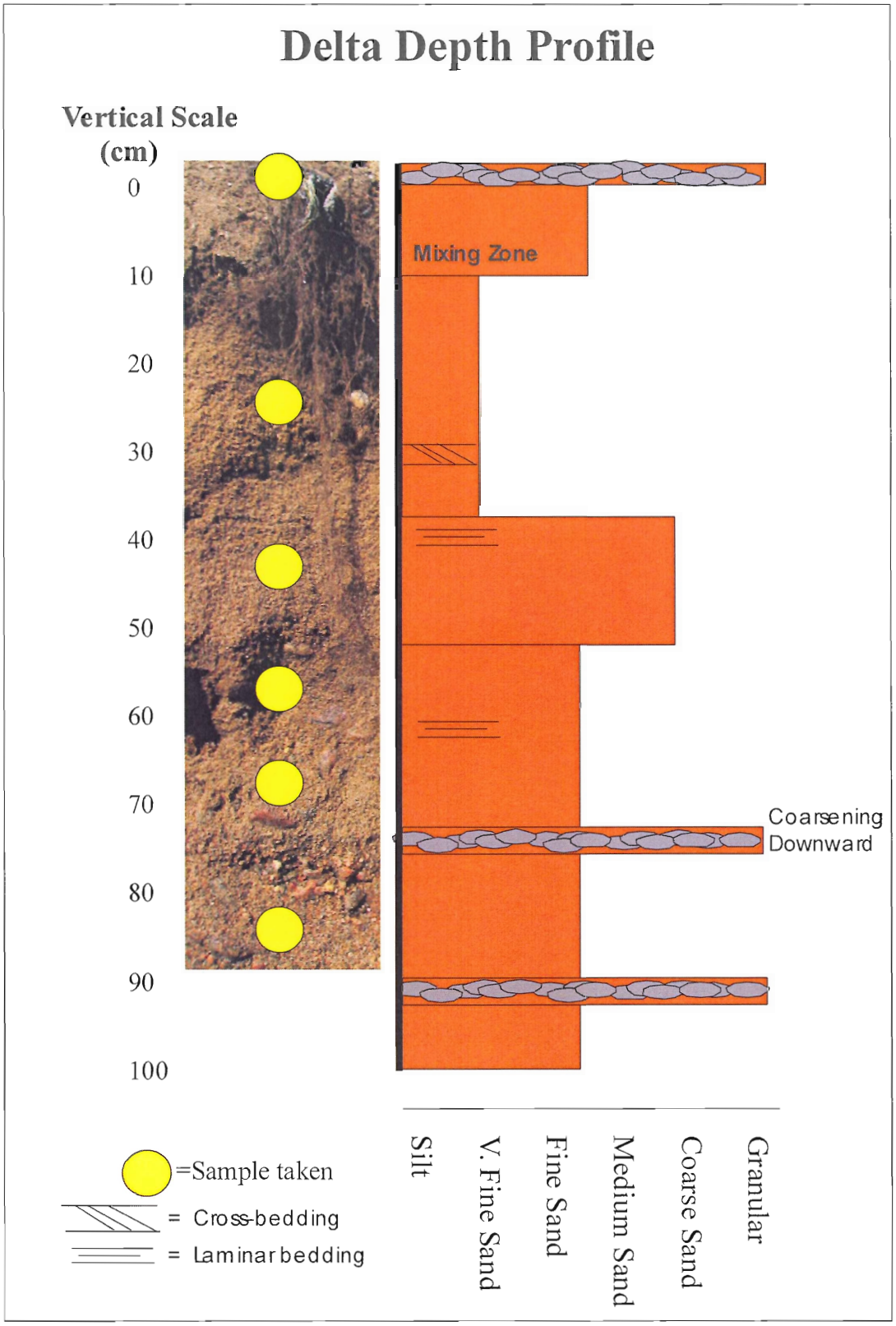


Figure 3.2: Schematic diagram of sampled wall of trench in glaciomarine delta with photo of profile. Units shown were generally laterally extensive along the 1.5 m trench.

### 3.2.2 Boulders on eskers

Sampling of boulders on eskers is different in that the material to be dated is cut and chiseled from the top of a solid boulder. It is best to sample multiple boulders, as it improves the reliability of the ages by allowing for more data to determine whether individual samples contain inheritance. In this study only two boulders (Figure 3.3) were sampled as they were the only suitable sample targets found after multiple days of helicopter surveys, as well as 4 days of searching on foot. The key to a good boulder sample is that the boulder is large, ideally greater than 1.5 m in height, that it has a flat top, and that it is located on the crest or highest point of the esker. The size of the boulder is important, because the larger the boulder, the less likely that it could be overturned following deposition. For TCN dating to provide an accurate date, the same surface of the boulder must be exposed to cosmic rays continuously since it was initially uncovered. A large boulder is much less likely to become covered in snow or sediment, which has the ability to shield the boulder surface from cosmic rays. It is also unlikely that boulder would have been post-depositionally exhumed. This assumption was made due to the very little erosion which occurs in the arctic, as well as field observations noting a lack of material that had seemed to have fallen down the esker slope. Having a flat top on the boulder allows for cosmic rays to equally bombard the surface rather than being self-shielded (placed in shadow) by an uneven surface. The location of the boulder at the crest of the knife-edge ridged esker suggests that the boulder was deposited directly on the esker and has not moved. Boulders on the flanks of the esker may have rolled there due to subsequent erosion and thus have not maintained the same orientation since deposition. Sampling of boulders was performed using a wet/dry portable 10" diamond

cutoff saw. Samples were obtained by cutting grooves into the top of the boulder, then using a chisel and rock hammer to break pieces out. The sample was taken from the center of the boulder; no sample material was taken within 10 cm from the edge of the boulder, and the material removed was 1.5-2 cm thick. In the case of the boulders there were no snow, erosion, geometry, or shielding corrections to be made.

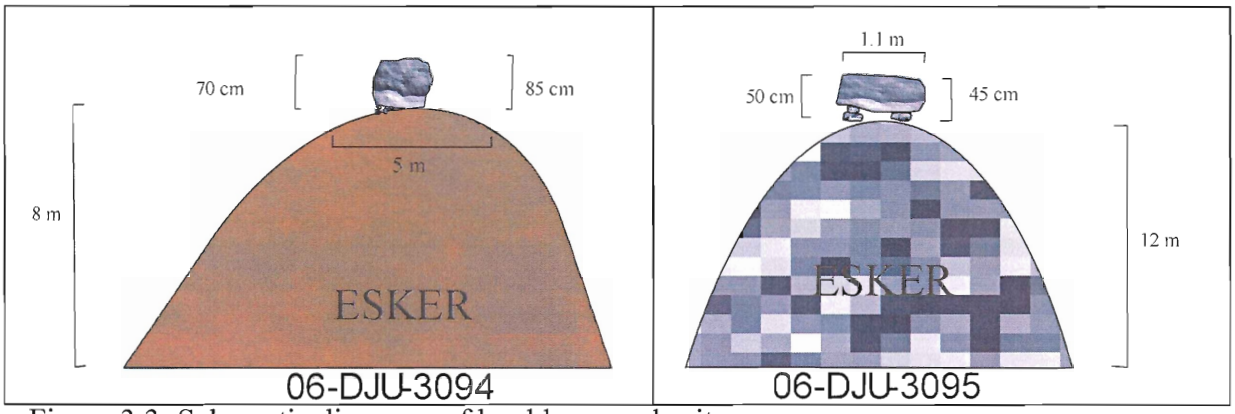

Figure 3.3: Schematic diagrams of boulder sample sites.

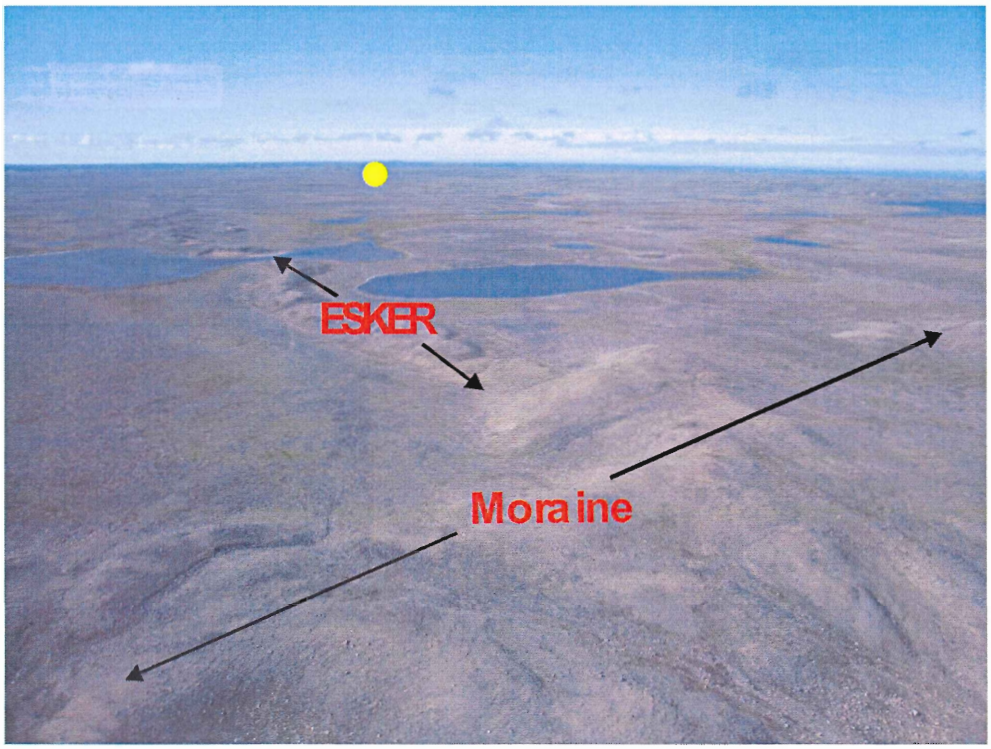

Figure 3.4: Esker-Kingnait moraine convergence sample site 06-DJU-3094 just off bottom of picture, 06-DJU-3095 sample site in distance (yellow dot) (S. Kelley Photo).

### 3.3 Physical and chemical processing

Physical and chemical processing is used to isolate quartz grains, and later the beryllium isotopes. Physical treatment consisted of utilizing both a jaw crusher for the breakdown of rock samples larger than 5 mm, as well as a disk pulverizer to break the sample down to the optimum 250-355 μm grain size, which is determined by sieving the crushed material through sieves of sizes 500 μm, 355 μm, and 250 μm. A final physical processing method employed in this study was the use of abrasion, in which crushed samples are subjected to high pressure air, causing physical agitation of the sample in a confined container. The purpose of this abrasion is to break down pre-softened non-quartz grains by causing grains to physically collide with one another, with quartz having a generally higher hardness than other gains present in the sample (hardness of 7 on the Mohrs hardness scale).

Next, chemical treatment was performed at the Cosmogenic Nuclide Exposure dating Facility (CNEF) at Dalhousie University. Chemical treatment is used to further break down and get rid of non-quartz containing material. Chemical treatment consists of placing the sieved material in series of acid baths: Aqua Regia (3HCL: $1HNO_3$), followed by HF to attempt to dissolve away the non-quartz minerals in the sample. Next, the sample is subjected to ultrasonics in an acid bath of HF to further separate non-quartz material from the sample, and partially dissolve the quartz to remove the outer layer of the quartz grains as they may be contaminated with atmospheric nuclides.

The next stage of chemical treatment is the dissolution of the quartz. In this step the purified sample is spiked with a known mass of BeCl ($^{9}$Be atoms) to provide a sufficient BeO target for accelerator mass spectrometry (AMS). The CNEF carrier is a

unique solution made from a beryl crystal extracted from >100 m depth in Wyoming. Its 6 year average $^{10}Be/^{9}Be$ is 4.5 x $10^{-15}$ at Lawrence Livermore National Lab AMS. This carrier is added gravimetrically. A chemistry process blank is created for every 7 samples analyzed. This contains only the carrier and deionized water and the acids that were previously added to the sample. The set of blanks and samples then were then dissolved in HF, HCl, and Aqua Regia, and then evaporated until only BeO remains.

The final step of the chemical treatment is anion and cation chromatography with a controlled precipitation step to isolate Be in the solution. The Be in BeCl form is precipitated using ultra pure ammonia gas to create BeOH. The precipitate was then baked at 850°C. (For further information on physical and chemical treatment see Appendix D) The entire chemical and physical procedure took eight weeks to perform.

### 3.3.1 Accelerated mass spectrometry

The remaining BeO powder was then packed with native niobium in special target holders for transport to Lawrence Livermore National Laboratories where AMS was performed. The mass spectrometer measures the ratio of $^{10}Be/^{9}Be$. These results are returned to CNEF where the amount of $^{10}Be$ is calculated using the equation below (Gosse and Philips, 2001).

$$^{10}Be = r\, m_c\, ( A / W_{Be} ) / m_{qtz}$$

Where:

$^{10}Be$ = concentration of $^{10}Be$ (atoms/g)

r = ratio of $^{10}Be/^{9}Be$

$m_c$ = mass of carrier

A = Avogadro's number

W = atomic weight of Be

$m_{qtz}$ = mass of quartz

## 4.0 Results

The following is the resulting TCN concentrations for samples taken (see Figure 4.1 below for sample locations).

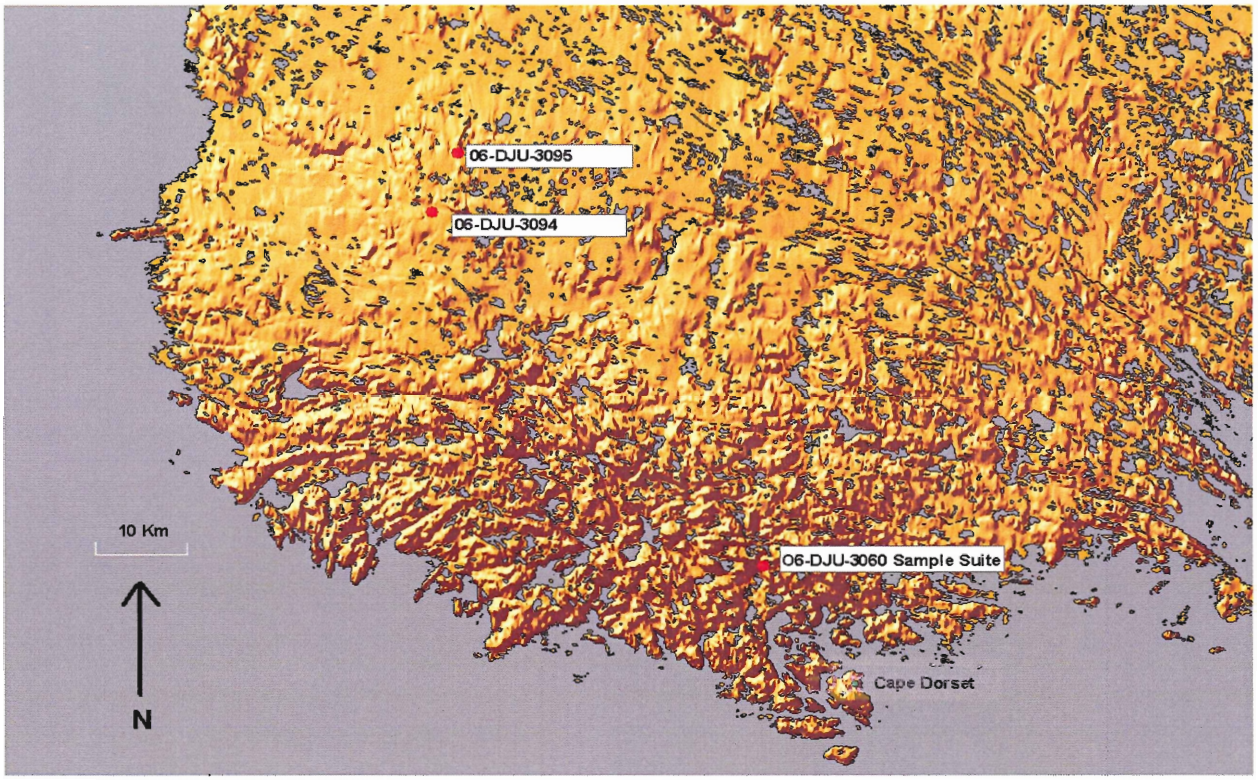


Figure 4.1: Map of the western Foxe Peninsula showing sample locations.

| CNEF ID | Sample ID | Sample type | Latitude (deg) | Longitude (deg) | Altitude (km) | Sample depth (cm) | Sample thickness (cm) |
|---|---|---|---|---|---|---|---|
| 1779 | Blank for 20061027 | BLANK | | | | | |
| 1912 | 06DJU 3060-1 | PEBBLES | 64.36N | 76.74 W | 0.151 | 0 | 2 |
| 1913 | 06DJU 3060-2 | SAND | 64.36N | 76.74 W | 0.151 | 27 | 3 |
| 1914 | 06DJU 3060-3 | SAND | 64.36 N | 76.74 W | 0.151 | 41 | 4 |
| 1915 | 06DJU 3060-4 | SAND | 64.36 N | 76.74 W | 0.151 | 56 | 4 |
| 1916 | 06DJU 3060-5 | SAND | 64.36 N | 76.74 W | 0.151 | 72 | 6 |
| 1917 | 06DJU 3060-6 | SAND | 64.36 N | 76.74 W | 0.151 | 90 | 4 |
| 1918 | 06DJU 3094 | BOULDER | 64.75 N | 74.54 W | 0.274 | 0 | 2 |
| 1780 | Blank for 20061028 | BLANK | | | | | |
| 1919 | 06 DJU-3095 | BOULDER | 64.81 N | 74.49 W | 0.234 | 0 | 2 |

Table 4.1: Sample sites, material sampled, and location and depth information

### 4.1 $^{10}$Be concentrations

Eight samples in total were analyzed; two from boulders perched on eskers, and six taken from a depth profile in a raised glaciomarine delta. These samples were processed with two chemical blanks. The chemical blanks had values of $6.56 \times 10^4$ $^{10}$Be atoms and $8.58 \times 10^4$ $^{10}$Be atoms. Both of these values are slightly above the average value of $5.50 \times 10^4$ $^{10}$Be atoms, suggesting that there is a small degree of $^{10}$Be contamination in the sample preparation or error in AMS. The total adjustment for $^{10}$Be/$^{9}$Be error was only 3.8%, and therefore any contaminant would have less than 1% effect on the age.

The boulder samples DJU-06-3094 and DJU-06-3095 had blank and background corrected abundances of $1.39 \times 10^6$ and $1.74 \times 10^6$ $^{10}$Be atoms respectively, which yields concentrations of $4.64 \times 10^3$ and $5.08 \times 10^3$ $^{10}$Be atoms $g^{-1}$ quartz.

Concentrations from the raised marine delta profile ranged from $2.82 \times 10^6$ to $1.39 \times 10^6$ $^{10}$Be atoms. This is a range of $4.62 \times 10^4$ $^{10}$Be atoms/g quartz to $2.55 \times 10^4$ $^{10}$Be atoms/g quartz. The $^{10}$Be concentration decreases with depth, due to decreased production below the surface (Fig. 5.2). From the concentration values found in samples taken, age determinations as well as adjustments can be made. Overall, the average blank concentration was only 0.4% of the average measured $^{10}$Be atoms in a depth profile sample, thus uncertainty in the blank contributes a negligible error to the age determination process.

| CNEF ID | SAMPLE ID | $^{10}Be/^{9}Be$ Corrected for B & Background | $^{10}Be/^{9}Be$ ERROR | $^{10}Be$ concentration $^{10}Be$ atoms ($10^6$) | $^{10}Be$ atom/ g quartz | $2\sigma$ Uncertainty ($10^6$ atoms) |
|---|---|---|---|---|---|---|
| 1779 | Blank for 20061027 | 4.825E-15 | 5.251E-16 | 0.07 | | |
| 1912 | 06DJU 3060-1 | 1.944E-13 | 6.241E-15 | 2.81 | $4.62 \times 10^4$ | 0.17 |
| 1913 | 06DJU 3060-2 | 1.722E-13 | 7.022E-15 | 2.41 | $4.00 \times 10^4$ | 0.19 |
| 1914 | 06DJU 3060-3 | 1.402E-13 | 3.884E-15 | 1.98 | $3.29 \times 10^4$ | 0.11 |
| 1915 | 06DJU 3060-4 | 1.356E-13 | 3.438E-15 | 1.91 | $3.18 \times 10^4$ | 0.09 |
| 1916 | 06DJU 3060-5 | 1.151E-13 | 3.100E-15 | 1.64 | $2.66 \times 10^4$ | 0.09 |
| 1917 | 06DJU 3060-6 | 1.119E-13 | 3.995E-15 | 1.53 | $2.55 \times 10^4$ | 0.11 |
| 1918 | 06DJU 3094 | 9.748E-14 | 2.817E-15 | 1.39 | $4.64 \times 10^4$ | 0.08 |
| 1780 | Blank for 20061028 | 6.165E-15 | 5.094E-16 | .09 | | 0.01 |
| 1919 | 06 DJU-3095 | 1.271E-13 | 3.354E-15 | 1.74 | $5.80 \times 10^4$ | 0.09 |

Table 4.2: TCN concentrations for the depth profile through the raised delta.

Standards used in AMS work
Assumed $^{10}Be$ half life = 1.5 ma
$^{10}Be/^{9}Be$ ratio for standard = $3.11 \times 10^{-12}$
Carrier background for standards = $4.0 \times 10^{-14}$
Boron correction factor = $8.0 \times 10^{-5} \pm 5.0$

## 5.0 Interpretation

### 5.1 Interpreting boulder concentrations as exposure ages

The dates for the boulder samples were 7.2 ka for 06-DJU-3094 and 9.8 ka for 06-DJU-3095. These values make sense for the regional glacial geology, though further data will be required to determine whether inheritance is present in the older boulder. It is impossible to determine the precise amount of inheritance present in a boulder, though through comparison to other data the presence of inheritance can be inferred for statistical outliers with higher than expected concentrations.

### 5.2 Interpreting the topset concentrations as exposure ages

The dates for the depth profile ranged from 8.0 ka to 13.0 ka, with the samples increasing with age as depth was increased. This relationship can be seen in Table 5.1 and indicates that the amalgamated samples of sand all had inheritance. This has a more significant effect on the ages of deeper samples due to their lower in situ concentrations.

| CNEF ID | Sample ID | Sample depth (cm) | Un-adjusted age (ka) |
|---|---|---|---|
| 1912 | 06DJU 3060-1 | 0 | 8.0 |
| 1913 | 06DJU 3060-2 | 27 | 9.6 |
| 1914 | 06DJU 3060-3 | 41 | 9.4 |
| 1915 | 06DJU 3060-4 | 56 | 10.8 |
| 1916 | 06DJU 3060-5 | 72 | 11.0 |
| 1917 | 06DJU 3060-6 | 90 | 13.0 |

Table 5.1: Table showing depth profiles unadjusted ages as they increase with depth.

### 5.3 Inheritance adjustments

The dates reported in the previous section were calculated without an adjustment for inheritance. Inheritance is the concentration of TCN in the sampled material which

was in place before the material was deposited. The dates reported above were calculated with the initial assumption that all of the TCN measured in the sample was produced in situ after deposition. In this section the concentration will be adjusted to reflect a more accurate age determination.

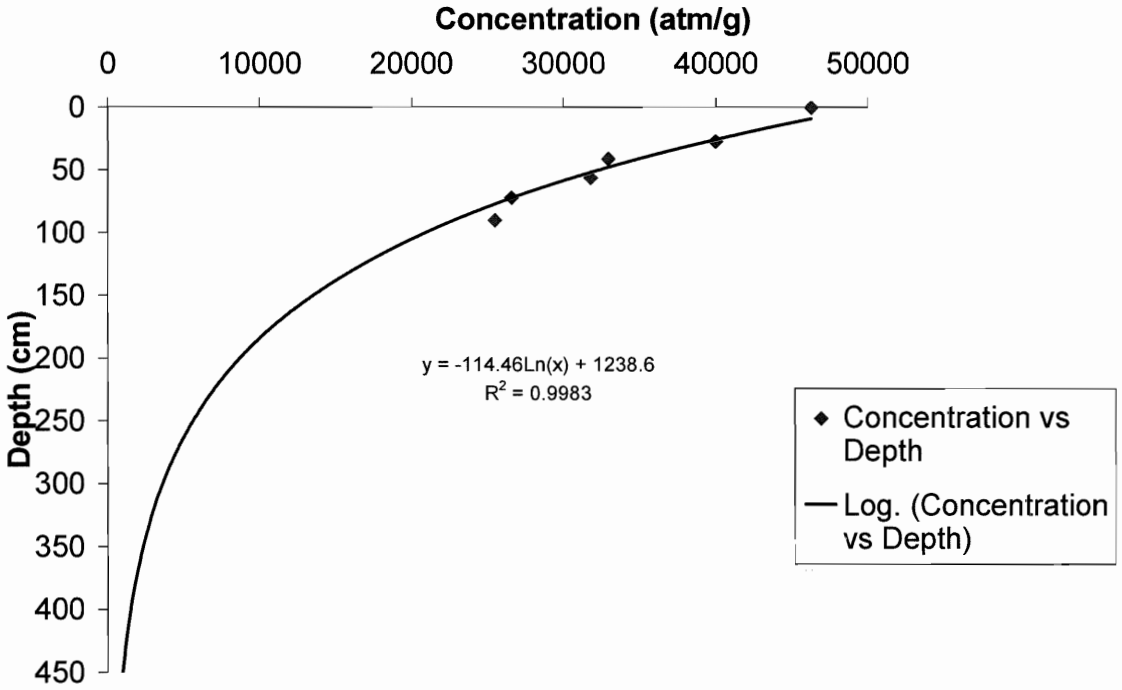


Figure 5.1: Plot of Concentration vs Depth for the depth profile samples. Curve represents a logarithmic regression function which was matched to the inheritance adjusted data with the curve being placed asymptotic to zero.

Inheritance was calculated through the minimization of a least squares regression of the profile ages. This reduced the difference between ages through the profile, removed the artificial age increase with depth. The inheritance value for the depth profile was 9676 atoms/g. The mean age for the depth profile is 7.5 $\pm$ 0.6 ka where the uncertainty is the standard error $\sigma / \sqrt{n}$ of the ages. For full depth profile results see in Table 5.2. In Table 5.3, a value of 9676 atoms/g was used based on a statistical

minimization of the 2σ error using the goal seek command in Microsoft excel, with extreme possible values ranged from 8000 atoms/g to 13000 atoms/g used in estimations of error.

| CNEF ID | Sample ID | Inheritance (atom/g) | Density | Erosion rate g/cm2 yr | Age (ka) | Inheritance/Concentration precision (2σ) |
|---|---|---|---|---|---|---|
| 1912 | 06DJU 3060-1 | 9676 | 2.7 | 0.0018 | 6.5 | 0.4 |
| 1913 | 06DJU 3060-2 | 9676 | 1.85 | 0.0027 | 7.7 | 0.6 |
| 1914 | 06DJU 3060-3 | 9676 | 1.85 | 0.0027 | 7.0 | 0.4 |
| 1915 | 06DJU 3060-4 | 9676 | 1.85 | 0.0027 | 8.0 | 0.4 |
| 1916 | 06DJU 3060-5 | 9676 | 1.85 | 0.0027 | 7.4 | 0.4 |
| 1917 | 06DJU 3060-6 | 9676 | 1.85 | 0.0027 | 8.6 | 0.6 |
| 1918 | 06DJU 3094 | 0 | 2.7 | 0.0000 | 6.9 | 0.4 |
| 1919 | 06 DJU-3095 | 0 | 2.7 | 0.0000 | 8.9 | 0.5 |

Table 5.2: Age as adjusted for inheritance as well as other adjustments.

### 5.4 Uncertainties

Total uncertainty in the TCN dates can be calculated by the equation below which is a combination of accuracy and precision:

$$\text{Uncertainty} = (\sum(\text{random error}^2 + \text{systematic error}^2))^{1/2} \quad \text{Eq. 4.1}$$

Systematic uncertainty is an uncertainty which limits accuracy due to a consistent altering of the data. In this study systematic uncertainty is involved in the estimation of production rates as well as possible variations in production rate, values regarding the carrier, or other calculation errors carried throughout the age interpretation.

Random error can have an affect on the precision and accuracy of the data though inconsistencies in individual measurements. In this study random error consists of inheritance adjustment, density estimates, sample thickness and depth measurements, location and elevation measurements, as well as adjustments for snow cover. See table 5.3 for calculation of error in age estimates.

### 5.4.1 Production rates

Production is defined to be the rate at which a nuclide is produced from a specified target measured in atom $g^{-1}$. Production rate is controlled by six factors: surface production, thickness of sample, topographic horizon, subsurface production, snow shielding, and geometry of the feature; each of these factors plays a role in controlling the final production rate. It is the final production rate that is used to determine the age of the sampled material and thus each factor contributes a degree of uncertainty, as shown in Table 5.3.

Surface production: The rate at which a nuclide is produced by GCR at a set latitude and elevation. Latitude is a factor as more GCR penetrate the Earth's magnetic field with higher latitude due to the dipole nature of the magnetic field. Also, the orientation of the field line orientation of the radiation becomes closer to parallel to the magnetic field at higher latitude, reflecting less GCR away. Elevation is a factor in surface production due to the amount of atmosphere the GCR has to pass through before encountering the surface, therefore at higher elevation there is less attenuation (apparent attenuation: g $cm^{-2}$). In Table 5.3, a value of 5.1 (Stone, 2001) was used the set value while an extreme value of 4.8 atoms/g/a (Gosse, 2007) was used. A small component of this is also due to muonic interactions with the target. Due to their lighter less reactive nature, muonic contribution becomes more of a factor as depth increases

Subsurface production: The production at depth due to decreasing cosmic ray flux with depth. This is a factor only for subaerial samples in which the number of GCR particles has decreased due to shielding of material lying above the sample.

Thickness of sample: The thickness of the taken sample allows for a production rate to be determined for the specific thickness sampled, which is found through the integration of concentration versus depth curve.

Topographic horizon: The shielding effect from surrounding topography. As a rule of thumb, hills with an azimuth less than 12.5° from the ground have a negligible affect on production.

Snow shielding: The shielding from GCR due to annual or permanent snow cover (See 5.4.2).

**5.4.2 Snow cover**

The nearest location for snow cover data to the study area is the town of Cape Dorset, located 15 km south of the raised delta and 60 km southeast of the esker sample sites. The climate record for Cape Dorset is recorded by Environment Canada, which has maintained a continuous presence at the weather station there from 1971 to 2000. The data from their archives was used to make an estimate of snow cover over the study area following deposition of the sampled materials. This snow cover value is then used to estimate the amount of shielding the sampled materials may have received from snow. Using average snow depths over the past 30 years in the region, a depth of 45 cm used as an approximate value for 6 months of snow cover during the year. Snow density was estimated at 0.2 g/cm$^3$, this value is the reported value for average snow density on the Arctic Ocean and thus will be used as an acceptable proxy for this study area (Warren, 1999; Environment Canada, 2006). In Table 5.3, a value of 6 months averaging 45 cm of snow at a density of 0.2 g/cm$^3$ was used for the set value, while extreme values ranged

from 5 months of snow at 40 cm depth at a density of 0.18 g/cm$^3$ to 6 months of snow at 55 cm depth with a density of 0.28g/cm$^3$.

## 5.5 Sensitivity analysis

### 5.51 Density adjustment

The density of the samples obtained plays a small yet important role in calculating an accurate exposure age. The assigned density for the boulder samples was 2.7 g/cm$^3$ as this is an accepted value for granitic gneisses. The density value of 2.7 g/cm$^3$ was also assigned to the pebbles that were collected at the top of the depth profile as they are of similar composition to that of the boulders. The subaerial portion of the profile was composed of medium grained sand and was assigned the density of 1.85 g/cm$^3$. This value was calculated through the minimization of the of a least squares regression of the profile ages, in the same manner that the inheritance was calculated. This value was also checked against known density values to check the validity of the calculated value. In Table 5.3, a value of 1.85 g/cm$^3$ was used the set value while extreme values ranged from 2- 1.7 cm a$^{-1}$.

### 5.5.2 Erosion adjustment

From field observations it is estimated that very little erosion has taken place. The boulders are of high density and showed no sign of spalling or fracture, and thus were considered un-eroded. The delta was also well preserved and showed no signs of major erosion at the sample site. The sedimentary structures in the sample pit were also well preserved, suggesting no to very little erosion had taken place. A rate of 0.005 cm a$^{-1}$ was estimated to account for minor erosion (37.5 cm) that may have taken place. This erosion rate was determined through the minimization of the of a least squares regression

of the profile ages, in the same manner that the inheritance and density were calculated. This low value is also supported by the presence of small scale features (less than 50 cm in height) that were still preserved on the delta surface, such as beach deposits left by falling sea level and lag deposits. In Table 5.3, a value of 0.005 cm $a^{-1}$ was used as the set value while extreme values ranged from 0.006 - .003 cm $a^{-1}$.

| Source of uncertainty | Age Range (ka) | % uncertainty |
|---|---|---|
| Surface production | 7.2 – 7.9 | 3.2% |
| Snow shielding | 7.5 – 7.7 | 1.3% |
| Inheritance | 6.3 - 8.2 | 12.6% |
| Density | 7.2 – 7.9 | 4.7% |
| Erosion rate | 7.4 – 7.7 | 6.0% |

Table 5.3: Calculations of uncertainty in age estimates. Age range is based on two extreme possibilities for that factor with all other factors remaining at the calculated set value, with the % uncertainty being the range divided by two divided by 7.5 ka.

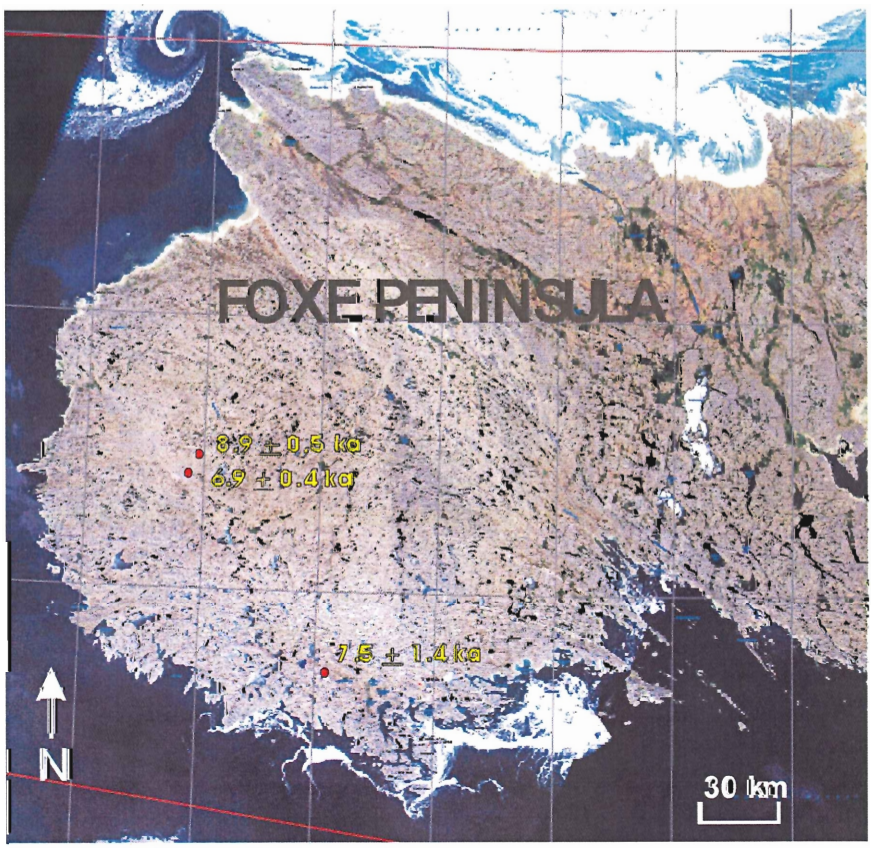


Figure 5.2 Map showing final ages and their locations.

## 6.0 Discussion and implications

### 6.1 Glacial dynamics implications

Dates derived from TCN exposure date indicate a deglaciation of the western Foxe Peninsula beginning at 7.5 $\pm$ 1.4 ka. Based on paleo-ice dynamics records, it is likely that deglaciation occurred first along the southern coast of the peninsula, followed by northward ice marginal retreat, roughly opposite to the initial flow.

The age of the abandonment of the glaciomarine delta at 7.5 ka implies the onset of retreat from the Hudson Strait occurred at 7.5 $\pm$ 1.4 ka. The ice margin retreated northward exposing the esker at 64.75° N,-77.54° W at 6.9 $\pm$ 0.4 ka. With the given uncertainties, these ages fall very close to one another, suggesting rapid retreat across the region between 7.5 and 6.9 ka at a rate of approximately 0.1km/a, as the precise timing can not be resolved given the precision of this data. The northern most esker boulder at 64.81° N,-77.49° W gave an age of 8.9 $\pm$ 0.5 ka, a date which is unreasonably too old for the local geochronology. More likely this is due to prior exposure of the boulder material creating inheritance for which the boulder age can not be corrected. It should also be noted that if a similar inheritance value to that of the deltaic material is applied to the 8.9 $\pm$ 0.5 ka boulder, the age would become 7.2 ka, fitting well with the deglaciation data for the area. Unfortunately, this value can not be used as a date, as there is no way to infer past exposure history on a single boulder. This does though add to supporting evidence that inheritance was correctly estimated for the deltaic sediments, as it is possible that boulders entrained in an ice sheet may have an exposure history that is roughly similar to that of the delta material.

Through TCN exposure dates calculated in this study some time constraints can be placed on the creation of the Kingnait Moraines. The Kingnait Moraines are likely younger than 8.9 ka, as the age of the older boulder provides a maximum time constraint of possible deposition. From observations studied in the field, the Kingnait Moraines are discontinuous in the region, and in many places seem to be overlain by glaciofluvial sediment, possibly related to further retreat following deposition. It is from these observations that an inference can be made that the Kingnait Moraines were created as part of a pause in ice retreat or minor re-advance, possibly linked to a cold event at approximately 7.1 ka (Keigwin and Jones, 1995; Andrews et al. 1999). This climate event had correct climatic environments for creating a positive or equilibrium glacial mass balance, which would result in a glacial advance or a pause in the retreat that was occurring. However, considering the volume of sediment comprising the moraine, it is more likely that the ice margin was responding to the 8200 or Noble inlet event.

### 6.2 Review of new TCN methods

As stated earlier, this is project served as testing ground for two developments in TCN exposure dating; an improved method for depth profile dating of a glaciomarine delta, and dating of boulders perched on esker crests. Depth profile dating has been attempted in the past (Hilchey, 2004; Brushett, 2005) with limited success, as both previous attempts experienced difficulties calculating inheritance which led to $^{10}$Be concentrations which did not match the expected pattern of decreased concentration with depth, or expected deglacial histories from other geochronologic techniques. In Hilchey's study, only single samples were collected from multiple glaciomarine deltas, thus providing one sample per feature, similar to the dating of boulders. This did not

allow for correction of age determinations for inheritance, and therefore provided dates that were too old given local deglacial histories of northern Baffin Island. In Burshett's study of glaciomarine deltas in southern Maine, depth profiles sampled through multiple foreset beds. In two out of three deltas sampled the foreset beds did not follow the theoretical curve of concentration vs. depth, perhaps because inheritance varied between layers, likely due to mixing of material eroded off of the topsets. As a result these deltas could not be dated.

The success of the current project demonstrates that depth profile dating of glaciomarine deltas is a viable dating method that should prove useful in dating features that are frequently devoid of material suitable for $^{14}C$ dating. Secondly the partial success of the esker dating technique marks a first in the scientific literature. Hopefully, this success will inspire others to continue refinement of this method, as it provides a possibility to examine in high precision a record of the retreat of an ice margin.

## 7.0 Conclusions and future work

The hypothesis that the Kingnait Moraines of the western Foxe Peninsula are of Cockburn age is improbable. Exposure ages both from boulders perched on esker crests as well as a depth profile through a glaciomarine delta indicate that glacial retreat across the area more likely occurred around 7.0-7.5 ka. The suggestion of Kingnait moraine creation earlier than the Cockburn age is furthered by a boulder date of 8.9 $\pm$ 0.5 ka. This date provides a maximum possible age for deposition of the landform, and is younger than the Cockburn age of 9.6 ka. The second boulder exposure age of 6.9 $\pm$ 0.4 ka is likely a more reasonable timing for the deposition of the Kingnait Moraines as it corresponds well to other local geochronologic data, such as the depth profile age of 7.5 $\pm$ 1.4 ka, as well as $^{14}C$ dates on marine shells from across the peninsula (Utting in press, 2007). Furthermore, the age range derived for the TCN exposure ages also rules out the possibility that the Kingnait Moraines are of Younger Dryas age (12.8-11.5 ka), however, considering uncertainty in the method it is possible that the Noble Inlet advance (8.9-8.4 ka) and the 8.2 ka cold period were responsible for creating of the Kingnait Moraines.

In addition to the original hypothesis, this study also made a significant contribution to the geochronologic record of Southwest Baffin Island. This is important because these dates will hopefully provide a framework from which a deglacial history for the region can be further expanded upon. This expansion is especially important due to the proximity of the Foxe Peninsula to both the Hudson Strait and the Foxe Basin, two critically important features to LIS ice dynamics in the region.

Finally, the hypothesis that a depth profile through topset beds of a glaciomarine delta would yield $^{10}Be$ concentrations representative of the retreat of an ice margin from

the region proved to be correct. This study is one of the first to demonstrate that direct dating of a glaciomarine delta is successful. This is a significant contribution to geochronologic techniques, as it allows for the dating of a feature normally devoid of datable carbon material. This also marks an important contribution to geochronologic techniques through the use of TCN exposure dates on eskers, another tool that will be useful in constraining the retreat of an ice margin.

The objectives of this study were a success, and the results of this work may be incorporated into other mapping projects in the future as well as other efforts to better constrain the timing of ice movement in the eastern Arctic. In further efforts it would be important to more thoroughly map out the extent of the Kingnait Moraines and determine using TCN exposure dating or other techniques to discovery whether these feature are can be correlated to other features in the Arctic.

# REFERENCES


Andrews, J. T., and J. D. Ives. ""Cockburn" Nomenclature and the Late Quaternary History of the Eastern Canadian Arctic." Arctic and Alpine Research 10.3 (1978): 617-33.

Andrews, J.T. et al., "Abrupt deglaciation events and Holocene palaeoceanography from high-resolution cores, Cartwright Saddle, Labrador Shelf, Canada." Journal of Quaternary Science 14.5 (1999) 383-397

Bell, R. Observations on the Geology, Mineralogy, Zoology, and Botany of the Labrador Coast, Hudson Strait and Bas. Part D VII ed. Geological and Natural History Survey and Museum of Canada:, 1895.

Bell, R. "A Survey in Baffinland, with Short Description of the Country." Geographical Journal 18 (1901)

Blake, W. Jr. "End Moraines and Deglacition Chronology in Northern Canada, with Special Reference to Southern Baffin Island." Geologic Survey of Canada (1966): 1-31.

Borgstrom, I., and J. Kleman. "Geomorphic Evidence for Late Glacial Ice Dynamics on Southern Baffin Island and in Outer Hudson Strait, Nunavut, Canada." Arctic and Alpine Research 33.3 (2001): 249-57.

Brushett, D. "The First Exposure Age for Raised Glaciomarine Deltas: Auburn Plains Delta, Southern Maine." Honnours Thesis Dalhousie University Earth Science Department, 2005.

Corrigan, D., D. J. Scott, and St. Onge. "Geology of the Northern Margin Fo the Trans-Hudson Orogen (Foxe Fold Belt), Central Baffin Island, Nunavut." Geologic Survey of Canda Current Research.C-23 (2001)

Dansgaard, W., et al. "Evidence for Past Climate Stability from 205 Kyr Ice-Core Record." Nature 264 (1993): 218-20.

Dyke, A. S., D. Giroux, and L. Robertson. "Paleovegetaion Maps of Northern America, 18000 to 1000 Bp." Geologic Survey of Canada open file 4682 (2006)

Environment Canada. "Canadian Climate Normals:1971-2000; Cape Dorset, Nunavut." Enviroment Canada. 2000. <www.climate.weatheroffice.ec.gc.ca>.

Gosse, J. C., and F. M. Phillips. "Terrestrial Cosmogenic Nuclides: Theory and Application." Quaternary Science Review 20 (2001): 1475-560.

Gosse, J. C. to Samuel Kelley. Personal communication about production rates (March 9, 2007). 2007.

Grafenstien, U. von Erlenkeuser, H., et al. "The Cold Event 8200 Years Ago Documented in the Oxygen Isotope Record of Precipitation in Europe and Greenland." Climate Dyanmics 42.2 (1998): 73-81.

Hilchey, A. "Holocene Deglaciation of the Ravn River Valley, Northern Baffin Island, Nunavut." Honnours Thesis: Dalhousie University Earth Science Department, 2004.

Hodgson, D. A. "Quaternary Geology of Western Meta Incognita Peninsula and Iqualit Area, Baffin Island." GSC Bulletin #582 (2005)

Jennings, A. E., et al. "Marine Evidence for the Last Glacial Advance Across Eastern Hudson Strait, Eastern Canadian Arctic." Journal of Quaternary Science 13.6 (1998)

Kaufman, D., et al. "Abrupt Early Holocene Ice Stream Advance at the Mouth of the Hudson Strait, Arctic Canada." Geology 21 (1993): 1063-6.

Keigwin, L. D. and Jones, G. A. "The marine record of deglaciation from the continental margin off Nova Scotia." Paleooceanography 10.6 (1995) 973-986

Lal, D. "In Situ-Produced Cosmogenic Isotope in Terrestrial Rocks." Annual review of Earth and Planetary Sciences 16 (1988): 355-88.

Long, A.J., et al. "Early Holocene history of the west Greenland Ice Sheet and the GH-8.2 event." Quaternary Science Reviews 25.9-10 (2006): 904-922

Lowell, T.V., et al. "Age verification of the Lake Gribben forest bed and the Younger Dryas Advance of the Laurentide Ice Sheet." Canadian Journal of Earth Sciences 36.3 (1999) 383-393

Miller, G. H., et al. "Ice-sheet dynamics and glacial history of southeastern most Baffin Island and outermost Hudson Strait." Quaternary Research 30 (1988), 116–136.

Miller, G. H., et al. "Holocene glaciation and climate evolution of Baffin Island, Arctic Canada." Quaternary Science Reviews 24.14-15 (2005) 1703-1721

Meese, D., et al. "Preliminary Depth-Age Scale of the GISP2 Ice Core." Cold Regions and Engineering Laboratory special report 94-1 (1994)

Reuther, A., et al. "Late Pleistocene Glacial Chronology of the Pietrele Valley, Retezat Mountains, Southern Carpathians Constrained by $^{10}$Be Exposure Ages and Pedological Investigations." Quaternary International (In Press 2006)

Smart, D. F., and Shea , M. A. (ed.). "Handbook of Geophysics and the Space Environment." Air Force geophysics laboratory, 1985. 29.

Stone, J. O. "Air Pressure and Cosmogenic Isotope Production." Journal of Geophysical Research (2001)

St-Onge, M. R., et al. "Upper and Lower Plate Juxtaposition, Deformation and Metamorphism during Crustal Convergence, Trans-Hudson Orogen (Quebec–Baffin Segment), Canada." Precambrian Research 93.1 (1999): 27-49.

Stuiver, M., and P. Reimer. CALIB. Vol. 5.0.2. Cambridge University:, 2005.

Stuiver, M., and P. Reimer. "Raidiocarrbon Calibration Program." Radiocarbon 53 (1993): 215-30.

K. C. Taylor, et al. "The Holocene-Younger Dryas Transition Recorded at Summit, Greenland." Science 278 (1997) 825-827.

Utting, D. J., et al. "Preliminary Ice-Flow History and Report on Surficial Studies, Foxe Peninsula, Southwest Baffin Island, Nunavut." Geologic Survey of Canda Current Research (2007 in press)

Warren, S. G., et al. "Snow Depth on Arctic Sea Ice." Journal of Climate 12 (1999)

**Appendix A**
**MORAINE/ ESKER CONFLUENCE**

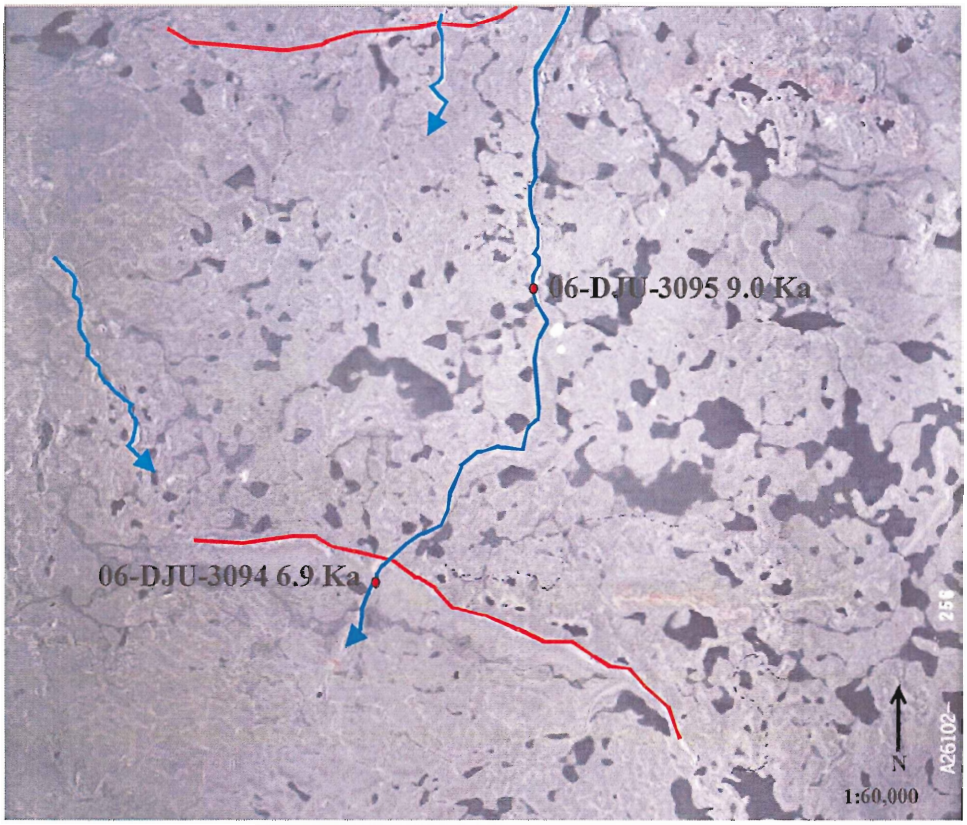


*Above:* Airphoto used for mapping, showing esker and moraines at sample sites.
*Below:* Photo of esker and moraine north of 06-DJU-3095 sample site. (air photo courtesy of C-NGO)


Helicopter
for scale
ESKER
Moraine

**Appendix B**
**AMS DATA**

| | DATE | | SAMPLE NAME | CAMS # | runs | | r_to_rstd | interror | exterror | Truefrac |
|---|---|---|---|---|---|---|---|---|---|---|
| Gosse | | 37590 | JG1779 | BE23064 | | 2 | 0.001532 | 0.000167 | 3.32E-05 | 0.826819 |
| Gosse | | 37590 | JG1912 | BE23065 | | 2 | 0.063254 | 0.001974 | 0.000849 | 0.978606 |
| Gosse | | 37590 | JG1913 | BE23066 | | 2 | 0.056191 | 0.002223 | 0.001324 | 0.988474 |
| Gosse | | 37590 | JG1914 | BE23067 | | 3 | 0.046039 | 0.001055 | 0.001222 | 0.991891 |
| Gosse | | 37590 | JG1915 | BE23068 | | 2 | 0.044584 | 0.001079 | 0.00084 | 0.991713 |
| Gosse | | 37590 | JG1916 | BE23069 | | 2 | 0.038073 | 0.00097 | 0.000144 | 0.989101 |
| Gosse | | 37590 | JG1917 | BE23070 | | 2 | 0.037055 | 0.0009 | 0.001257 | 0.987904 |
| Gosse | | 37590 | JG1918 | BE23071 | | 2 | 0.032478 | 0.000879 | 0.000141 | 0.988279 |
| Gosse | | 37590 | JG1780 | BE23072 | | 3 | 0.001957 | 0.000162 | 0.000135 | 0.834239 |
| Gosse | | 37590 | JG1919 | BE23079 | | 2 | 0.042316 | 0.001052 | 0.000385 | 0.985228 |
| Gosse | | 37590 | JG1780 | BE23072 | | 3 | 0.001957 | 0.000162 | 0.000135 | 0.834239 |

**AMS DATA** continued

| SAMPLE NAME | 10Be/9Be RATIO | ERROR | ( CORRECTED FOR BORON) RATIO | ERROR | 10Be/9Be RATIO (SAMPLE BKGD) RATIO | ERROR | 10Be/9Be RATIO (CORR. FOR BKGDS) % UNCERTAINTY | | COMMENTS |
|---|---|---|---|---|---|---|---|---|---|
| JG1779 | 4.83E-15 | 5.25E-16 | | | 4.83E-15 | 5.25E-16 | 0.108819 | KNSTD3110 | |
| JG1912 | 1.99E-13 | 6.22E-15 | 4.82549E-15 | 5.2511E-16 | 1.94E-13 | 6.24E-15 | 0.032102 | KNSTD3110 | very low current |
| JG1913 | 1.77E-13 | 7E-15 | 4.82549E-15 | 5.2511E-16 | 1.72E-13 | 7.02E-15 | 0.040783 | KNSTD3110 | very low current |
| JG1914 | 1.45E-13 | 3.85E-15 | 4.82549E-15 | 5.2511E-16 | 1.4E-13 | 3.88E-15 | 0.027702 | KNSTD3110 | |
| JG1915 | 1.4E-13 | 3.4E-15 | 4.82549E-15 | 5.2511E-16 | 1.36E-13 | 3.44E-15 | 0.025353 | KNSTD3110 | |
| JG1916 | 1.2E-13 | 3.05E-15 | 4.82549E-15 | 5.2511E-16 | 1.15E-13 | 3.1E-15 | 0.026929 | KNSTD3110 | |
| JG1917 | 1.17E-13 | 3.96E-15 | 4.82549E-15 | 5.2511E-16 | 1.12E-13 | 3.99E-15 | 0.035698 | KNSTD3110 | |
| JG1918 | 1.02E-13 | 2.77E-15 | 4.82549E-15 | 5.2511E-16 | 9.75E-14 | 2.82E-15 | 0.028901 | KNSTD3110 | |
| JG1780 | 6.16E-15 | 5.09E-16 | | | 6.16E-15 | 5.09E-16 | 0.082626 | KNSTD3110 | |
| JG1919 | 1.33E-13 | 3.32E-15 | 6.16455E-15 | 5.0936E-16 | 1.27E-13 | 3.35E-15 | 0.026382 | KNSTD3110 | |
| JG1780 | 6.16E-15 | 5.09E-16 | | | 6.16E-15 | 5.09E-16 | 0.082626 | KNSTD3110 | |

**APPENDIX C**

*Above:* view of glaciomarine delta from the southeast. Helicopter center of picture for scale. *Below:* Depth profile sample pit, with possible meltwater channel in background.

# WS4_QtzDissolution

***This worksheet outlines the steps for dissolving quartz and adding Be carrier.***

JG/GY

**Chemist:** GY

form:mm/dd/yy

**Date:** 10/27/06

| | 1 | 2 | 3 | 4 | 5 | 6 | 7 | 8 |
|---|---|---|---|---|---|---|---|---|
| **CNEF ID** | 1912 | 1913 | 1914 | 1915 | 1916 | 1917 | 1918 | 1779 |
| **Sample ID** | 06DJU 306-1 | 06DJU 3060-2 | 06DJU 3060-3 | 06DJU 3060-4 | 06DJU 3060-5 | 06DJU 3060--6 | 06DJU 3094 | Blank for 20061027 |
| **300 ml vessel ID** | B1 | B2 | B3 | B4 | B5 | B6 | B7 | B8 |
| **Beryl Carrier ID** | | | | | | | | |
| | (tare balance after each measurement) | | | | | | | |
| **Mass 300 ml vessel** | | | | | | | | 150.2128 |
| **Mass 40g quartz** | 60.8628 | 60.3647 | 60.0835 | 60.1784 | 61.6635 | 60.0218 | 30.0338 | 0 |
| **Mass Be carrier** | 0.2254 | 0.2182 | 0.2198 | 0.2196 | 0.2220 | 0.2131 | 0.2224 | 0.2118 |

**SAVE AS:** **C:/Chemistry/CHEM_WK YYMMDD .xls** **then PRINT**

- ☐ 1 Add 20 ml conc. HF and 2 ml $HClO_4$ per 5 g of quartz
- ☐ 2 Add 5 ml Aqua Regia
- ☐ 3 Heat at 100-125° C until quartz dissolves, add HF if needed
- ☐ 4 Raise to 200° C and evaporate to dryness
- ☐ 5 Add 5 ml $HClO_4$ and evaporate to dryness
- ☐ 6 Add 8 to 10 ml conc. $HNO_3$, swirl, and evaporate to dryness
- ☐ 7 Dissolved dried sample in 20 ml of 2% HCl

Comments

Sam Kelley Baffin

# WS5_ICP Aliquot and Al spiking

***This worksheet outlines the steps for collecting ICP aliquots and adding Al carrier.***

GY

**Chemist:** GY/AR

form: 02/17/01

**Date:** 12/04/01

☐ 1 **Label one 10 ml volumetric flasks per sample (16)**

☐ 2 **Label one ICP vial with CNEF ID per sample (16)**

| | B1 | B2 | B3 | B4 | B5 | B6 | B7 | B8 |
|---|---|---|---|---|---|---|---|---|
| CNEF ID | 1912 | 1913 | 1914 | 1915 | 1916 | 1917 | 1918 | 1779 |
| Sample ID | 06DJU 306-1 | 06DJU 3060-2 | 06DJU 3060-3 | 06DJU 3060-4 | 06DJU 3060-5 | 06DJU 3060--6 | 06DJU 3094 | Blank for 20061027 |
| Al carrier ID | | | | | | | | |
| Quant-EM est. Al in qtz | | | | | | | | |
| Volume carrier to add to smpl | | | | | | | | |
| Volume carrier to add to vol A | | | | | | | | |
| Volume carrier to add to vol. B | | | | | | | | |
| | Tare between mass measurements | | | | | | | |
| Mass100 ml volumetric | | | | | | | | |
| 100ml volumetric+sample+2%HCl | | | | | | | | |
| Mass 5 ml smpl pipetted to vol A | | | | | | | | |
| Bring up to 10 ml by 2%HCl | | | | | | | | |
| Mass 10 ml Sample to Vial B | | | | | | | | |
| Final Mass of 100 ml vol and smpl | | | | | | | | |
| Mass Al carrier to remaining (row18) | | | | | | | | |
| Unaccounted mass | | | | | | | | |

☐ 3 Get digestion vessel and cover ready, Do not wipe now.

☐ 4 Transfer the 90 ml sample back into vessel

☐ 5 Bring contents of volumetrics A and B to 10 ml

☐ 6 Transfer contents volumetrics to ICP vials with same number

# WS6_Anion Column Chemistry

***This worksheet outlines the steps for the Anion Column Chemistry***

**Chemist:** GY **Date:** form: MM/DD/YY

**Print this page**

- ☐ 1 Evaporate 80 ml to dryness at 100-120°C (will take at least 3 hrs)
- ☐ 2 Dissolve in 10 ml 9N HCl (let stand for several hours)
- ☐ 3 Transfer to 15 ml centrifuge tubes, rinse digestion vessels with 9N HCl to bring volume in tube to 10 ml
- ☐ 4 Centrifuge at 1500 rpm or higher for minimum of 10 minutes
- ☐ 5 Allow any 9 N HCl in columns to drain out; discard

| Column ID | A | B | C | D | E | F | G |
|---|---|---|---|---|---|---|---|
| Vessel | B1 | B2 | B3 | B4 | B5 | B6 | B7 |
| CNEF ID | 1912 | 1913 | 1914 | 1915 | 1916 | 1917 | 1918 |
| Sample ID | 06DJU 306-1 | 06DJU 3060-2 | 06DJU 3060-3 | 06DJU 3060-4 | 06DJU 3060-5 | 06DJU 3060--6 | 06DJU 3094 |

- ☐ 6 With stopcock closed, pipet sample (avoid residue)onto columns.
- ☐ 7 Collect sample in same (wiped)120 ml teflon vessel
- ☐ 8 Elute with 30 ml 9 N HCl, and collect that, close stopcock
- ☐ 9 5 ml 4.5 N HCl, collect Anion Supernate in labeled 100 ml bottle
- ☐ 10 100 ml 1 N HCl, collect Anion Supernate
- ☐ 11 50 ml deionized water. Discard.
- ☐ 12 **CONDITION ANION COLUMN**

(bottle A1) 50 ml 1N HCl, discard
(bottle A2) 50 ml 4.5 N HCl, discard
(bottle A3) 100 ml 9 N HCl, discard, but retain acid approx. 2 mm above resin

Comments

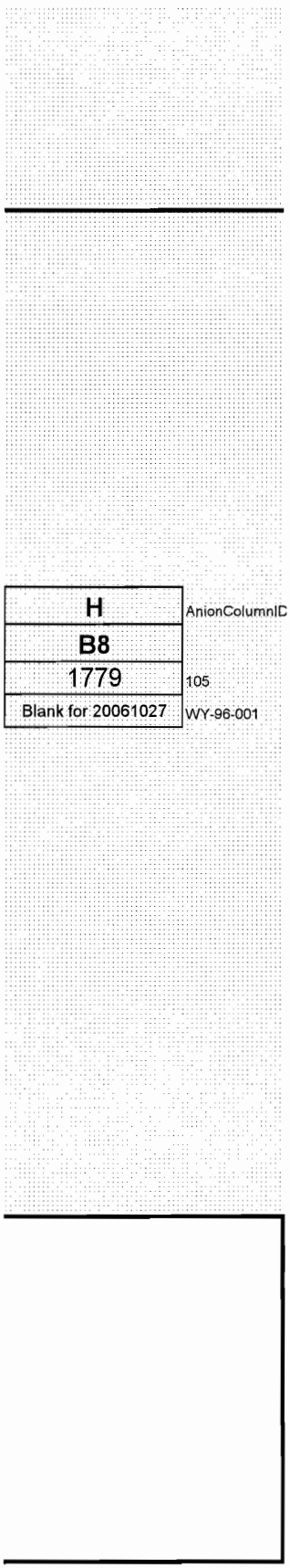
H
AnionColumnID
B8
1779
105
Blank for 20061027
WY-96-001

# WS7_Controlled Precipitate

***This worksheet outlines the steps for the controlled precipitation chemistry***

**Chemist:** GY **Date:** form: MM/DD/YY

**Print this page**

- ☐ 1 Evaporate "anion" elute to dryness at 125°C
- ☐ 2 Dissolve in 10 ml of a 1:1 solution of 0.5N HCl and 2% $NH_4Cl$
- ☐ 3 Transfer to 15 ml centrifuge, centrifuge for 10 minutes
- ☐ 4 Decant into clean test tube, heat in water bath at 60°C
- ☐ 5 Add drops of 1:1 $NH_4OH$:$H_2O$ to pH=9.2 (5 drops first then single)
- ☐ 6 Centrifuge for 15 minutes
- ☐ 7 Check pH of liquid, if less than pH=7, redo step ☐ 5
- ☐ 8 Decant, save with Anion Supernate
- ☐ 9 Wash with deionized water, vortex, centrifuge, decant
- ☐ 10 Wash with deionized water, vortex, centrifuge, decant
- ☐ 11 Wash with deionized water, vortex, centrifuge, decant

| | | | | | | | | | |
|---|---|---|---|---|---|---|---|---|---|
| **CNEF ID** | 1912 | 1913 | 1914 | 1915 | 1916 | 1917 | 1918 | 1779 | ## |
| **Vessel** | B1 | B2 | B3 | B4 | B5 | B6 | B7 | B8 | |
| **Sample ID** | 06DJU 306-1 | 06DJU 3060-2 | 06DJU 3060-3 | 06DJU 3060-4 | 06DJU 3060-5 | 06DJU 3060--6 | 06DJU 3094 | Blank for 20061027 | |
| **Approx. vol. Ptte** | | | | | | | | | |

Comments

# WS8_Cation Column Chemistry

*This worksheet outlines the steps for the Cation Column Chemistry*

**Chemist:** GY/JG _____ **Date:** mm/dd/yy _____

**Print this page**

☐ 1 Dissolve in 5 ml conc. HCl and evaporate to dryness at 125°C

☐ 2 Redissolve in 2.5 ml 1N HCl and 2.5 ml 0.5 N HCl

☐ 3 Transfer to centrifuge tube, rinse with 1 ml 0.5N, and centrifuge

| Column ID | 1 | 2 | 3 | 4 | 5 | 6 | 7 |
|---|---|---|---|---|---|---|---|
| Vessel | B1 | B2 | B3 | B4 | B5 | B6 | B7 |
| CNEF ID | 1912 | 1913 | 1914 | 1915 | 1916 | 1917 | 1918 |
| Sample ID | 06DJU 306-1 | 06DJU 3060-2 | 06DJU 3060-3 | 06DJU 3060-4 | 06DJU 3060-5 | 06DJU 3060--6 | 06DJU 3094 |

☐ 4 Pipette all of the sample into designated conditioned cation column

☐ 5 Discard the eluant. Add 220 ml 0.5 N HCL (bottle C6)

☐ 6 Collect eluant as Cation Supernate, add 200 ml 0.5 N HCl (bottle C7)

☐ 7 Collect eluant as Be-Sample into vessels.

☐ 8 Add 30 ml 1N HCl (bottle8)

☐ 9 Save this as Be-sample as well.

☐ 10 Add 100 ml 4.5 N HCl, save as Al sample.

☐ 11

☐ 12

☐ 13 **CONDITION CATION COLUMN**

(bottle C1) 100 ml 9N HCl
(bottle C2) 50 ml 4.5 N HCl
(bottle C3) 50 ml 1 N HCl
(bottle C4) 50 ml water
(bottle C5) 100 ml 0.5 N HCl

| |
|---|
| **8** |
| **B8** |
| 1779 |
| Blank for 20061027 |

# WS9_Be Sample Chemistry

***This worksheet outlines the steps to prepare the BeO sample***

**Chemist:** GY **Date:** form: mm/dd/yy

**Print this page**

☐ 1 Evaporate Be Sample from column in wiped digestion vessels at 125°C

☐ 2 Add 2-5 ml 20% perchloric and evaporate at 200oC

☐ 3 Again, add 2-5 ml 20% perchloric and evaporate at 200°C

☐ 4 Dissolve sample in 10 ml of 0.5 N HCl (optima grade)

☐ 5 Transfer to 15 ml centrifuge tube

☐ 6 Centrifuge and decant into clean centrifuge tube

☐ 7 Heat centrifuge tubes in water bath at 60°C

☐ 8 Precipitate $Be(OH)_2$ using Matheson ultimate grade ammonia gas

Gently bubble $NH_3$ with clean pipet tip on hose

for ca.15 bubbles, or ca. 8-12 sec until ptte forms

Optimum pH=9.2; 1N HCl may be added

☐ 9 Centrifuge 15 min., decant (save and redo ☐ 8 if pH of liquid is < 8)

☐ 10 Wash with water, vortex, centrifuge for 10 min, and decant

☐ 11 Record mass quartz vials, label, and place them in furnace holder

| CNEF ID | 1912 | 1913 | 1914 | 1915 | 1916 | 1917 | 1918 | 1779 | 105 |
|---|---|---|---|---|---|---|---|---|---|
| Vessel | B1 | B2 | B3 | B4 | B5 | B6 | B7 | B8 | |
| Sample ID | 6DJU 306- | 5DJU 3060 | 6DJU 3060 | 6DJU 3060 | 5DJU 3060 | DJU 3060- | 6DJU 309- | k for 2006 | WY-96-001 |
| Mass Qtz Vial | 2.4048 | 2.3832 | 2.3583 | 2.4398 | 2.3735 | 2.4021 | 2.4324 | 2.4273 | 2.1400 g |
| Mass Vial+Spl | 2.4056 | 2.3837 | 2.3896 | 2.4406 | 2.3741 | 2.4025 | 2.4329 | 2.4276 | 2.1410 g |
| Mass Spl | 0.0008 | 0.0005 | 0.0313 | 0.0008 | 0.0006 | 0.0004 | 0.0005 | 0.0003 | 1 mg |

☐ 12 Add 1 small drop of water with micropipet, slurry precipitate

☐ 13 Transfer sample into quartz vial, cover with alumina vial

☐ 14 Heat in oven at 120°C for 2-3 hours

☐ 15 Let cool and scrape sample down from walls of quartz tube

☐ 18 Place in furnace. Convert to BeO in furnace at 850°C for minimum 1 hr

☐ 19 Determine mass of vial + sample